ARR No. 4K03

NATIONAL ADVISORY COMMITTEE FOR AERONAUTICS

WARTIME REPORT

ORIGINALLY ISSUED

December 1944 as
Advance Restricted Report 4K03

WALL INTERFERENCE IN A TWO-DIMENSIONAL-FLOW WIND TUNNEL WITH CONSIDERATION OF THE EFFECT OF COMPRESSIBILITY

By H. Julian Allen and Walter G. Vincenti

Ames Aeronautical Laboratory
Moffett Field, California

NACA

WASHINGTON

NACA ARR No. 4K03

NATIONAL ADVISORY COMMITTEE FOR AERONAUTICS

ADVANCE RESTRICTED REPORT

WALL INTERFERENCE IN A TWO-DIMENSIONAL-FLOW WIND TUNNEL, WITH CONSIDERATION OF THE EFFECT OF COMPRESSIBILITY

By H. Julian Allen and Walter G. Vincenti

SUMMARY

Theoretical tunnel-wall corrections are derived for an airfoil of finite thickness and camber in a two-dimensional-flow wind tunnel. The theory takes account of the effects of the wake of the airfoil and of the compressibility of the fluid, and is based upon the assumption that the chord of the airfoil is small in comparison with the height of the tunnel. Consideration is given to the phenomenon of choking at high speeds and its relation to the tunnel-wall corrections. The theoretical results are compared with the small amount of low-speed experimental data available and the agreement is seen to be satisfactory, even for relatively large values of the chord-height ratio.

INTRODUCTION

The need for reliable wind-tunnel data for the design of high-performance aircraft has led in recent years to attempts to make the conditions of the tunnel tests conform more closely with the conditions prevailing in flight, especially with regard to the Reynolds and Mach numbers. Because of practical limitations in size and power, most existing wind tunnels, whether high speed or low speed, are not capable of providing full-scale Reynolds numbers for all flight conditions. In order to obtain the highest Reynolds numbers possible under the circumstances, it is necessary to use models dimensions of which are as large as possible relative to the cross-sectional dimensions of the tunnel test section. The effect of such large size is to make the test conditions depart further from the conditions prevailing in

flight by increasing the magnitude of the tunnel-wall interference. In the case of tests at high Mach numbers, the interference is increased still further by the tendency of the flow pattern of a compressible fluid, if unrestrained, to expand as the Mach number of the undisturbed stream increases. Since the walls of a closed-throat tunnel restrain certain of the streamlines at a fixed distance from the model, this expansion is prevented, and the tunnel-wall interference and corrections become progressively larger as the Mach number increases. The results obtained in the tunnel must therefore be corrected accurately for the effects of wall interference if they are to be applied with confidence to the prediction of free-flight characteristics.

In tests at high Mach numbers an additional complication arises. The effect of a model in a closed-throat tunnel may, in a sense, be thought of as equivalent to that of a constriction in the throat of the tunnel. The resulting converging-diverging nozzle formed by the model and the tunnel walls then has roughly the same characteristics at high speeds as the usual supersonic nozzle; that is, for some Mach number less than unity in the undisturbed stream, sonic velocity is reached at all points across a section of the tunnel at the position of the model, and the flow in the diverging region downstream of this section becomes supersonic. When this occurs, increased power input to the tunnel has no effect upon the velocity of the stream ahead of the model, the additional power serving merely to increase the extent of the supersonic region in the vicinity of the model. At this point the tunnel is said to be "choked" and no further increase in the test Mach number can be obtained. The value of the Mach number at which choking occurs is thus of extreme importance, since it determines the upper limit of the range of Mach numbers which can be obtained with a given combination of model and tunnel.

In testing airfoils to obtain section characteristics at subsonic speeds, it has become common practice in modern closed-throat wind tunnels to have the model span the tunnel so that supporting struts and their accompanying interference effects are entirely eliminated. If the tunnel has a cross section of rectangular shape, this arrangement results in a flow which is essentially two-dimensional.

The wall interference for such a two-dimensional-flow wind tunnel has been the subject of numerous investigations, the results

in general being expressible as series in ascending powers of (c/h), where c is the chord of the airfoil and h the height of the tunnel. The effect of wall interference upon the flow of an ideal fluid about a symmetrical airfoil at zero angle of attack is determined to the order $(c/h)^2$ by Lock in reference 1 and by Glauert in reference 2. The interference for an infinitesimally thin, cambered airfoil at a small angle of attack in an ideal fluid is given by Glauert to the order $(c/h)^2$ in reference 2, and investigations for the special case of a flat plate have been carried out to a higher order of accuracy by several writers. While the present report was being prepared, work by Goldstein appeared (references 3 and 4) in which the interference is determined to the order $(c/h)^4$ for a general cambered airfoil of finite thickness in an incompressible fluid, no restriction being made in the general results as to the magnitude of the camber, thickness, and the force coefficients. A still later paper by Goldstein and Young (reference 5) gives the modifications necessary in the previous results to allow for the effect of fluid compressibility to the order $(c/h)^2$.

In the present paper, the tunnel-wall corrections are determined to the order $(c/h)^2$ for the general airfoil in a compressible fluid for Mach numbers below that at which choking occurs. It is assumed that the thickness and camber of the airfoil are small and that the interference velocities are everywhere small as compared with the velocity of the undisturbed stream. A discussion is also included of the Mach number at which choking occurs. The various results presented are of essentially the same nature as those which already have appeared separately in the reference cited, but the methods of development and certain of the final results are different, especially with regard to the interference associated with lift. The validity of the final corrections is examined by comparison with the available experimental data. The equations also are compared with the results of references 3, 4, and 5, and the afore-mentioned differences are discussed.

The discussion is limited to airfoils placed midway between the upper and lower walls of the tunnel. Mathematical symbols are defined as introduced in the text. For reference, a list of the more important symbols and their definitions is given in appendix B.

DEVELOPMENT OF CORRECTION EQUATIONS

In an analysis of tunnel-wall interference it is desirable to look upon the theoretical development of the tunnel-wall corrections as consisting of two parts. First, it is necessary to determine the manner and extent to which the tunnel walls alter the field of flow about the airfoil from what it would be if they were not present. Second, it is necessary to calculate the effect of these alterations upon the measured characteristics of the airfoil. The development of the correction equations of this report has been divided into those two general sections.

In reference 6, the use of the method of superposition to determine the pressure distribution over the surface of an airfoil section in free air is presented. It is shown that in the calculation of the flow at the surface of a thin airfoil of small camber, the effects of camber and thickness may be considered independently. This follows directly from the fact that the velocities induced by the vortex sheet used to represent camber and those induced by the source-sink system used to represent thickness are simply additive in their effect on the flow over the airfoil.

To treat the problem of wall interference, it is again convenient to consider the thickness and camber effects separately. The flow changes associated with airfoil thickness are found by considering the interaction between the tunnel walls and the base profile of the airfoil, the base profile being defined as the profile the airfoil would have if the camber were removed and the resulting symmetrical airfoil placed at zero angle of attack. The interference effects associated with airfoil camber are found by analyzing the interaction between the tunnel walls and an infinitesimally thin airfoil having the same camber as the actual airfoil. In addition to the interference effects associated with airfoil thickness and camber, it is necessary to consider a further alteration of the field of flow caused by the confining influence of the tunnel walls upon the airfoil wake. When the individual effects promoted by the interference between the walls and the airfoil thickness, camber, and wake are known, the total alteration in the flow at the airfoil is found by superposition, and the characteristics of the airfoil in the altered field of flow are compared with the characteristics in free air. This comparison leads to simple formulas which enable the prediction of the free-flight characteristics when the characteristics in the tunnel are known.

The method of superposition, which is fundamental to the entire analysis, is in general inapplicable to compressible flow as the differential equation for such flow is nonlinear in the physical plane. The separate solutions which are superposed are obtained, however, by assuming that the airfoil is of small thickness and camber and that the induced velocities are thus small as compared with the velocity of the undisturbed flow. On the basis of this assumption the equation of compressible flow becomes a linear differential equation - namely, Laplace's equation (references 7, 8, and 9) - so that superposition of velocities is, in this case, technically permissible. Furthermore, the tunnel-wall corrections are in most cases rather small relative to the experimental quantities being corrected, so that it is not thought that the use of this approximate method will lead to large errors in the final corrected quantities.

Influence of Tunnel Walls upon Field of Flow at Airfoil

Thickness effect.- The interaction between the base profile and the walls of a two-dimensional-flow tunnel has been considered by Lock for the case of an incompressible fluid (reference 1; a discussion of Lock's method is also given by Glauert in reference 2). Lock's method of analysis is essentially to introduce an infinite series of images of the base profile such as to satisfy the condition that there is no flow normal to the walls, to replace each image by a suitable source-sink doublet, and to calculate the velocity induced at the base profile by this system of doublets. It is shown that the net effect of the tunnel walls upon the flow at the base profile is to increase the effective axial velocity of an incompressible stream by the amount

$$(\Delta_1 V')_i = \Lambda \sigma V' \tag{1}$$

where

V' apparent stream velocity at airfoil as determined from measurements taken at a point far ahead of model

σ a factor dependent upon size of airfoil relative to tunnel

Λ a factor dependent upon shape of base profile

The factor σ is defined by the equation

$$\sigma = \frac{\pi^2}{48}\left(\frac{c}{h}\right)^2 \tag{2}$$

where (c/h) is the ratio of the airfoil chord to the tunnel height. The factor Λ can be determined for any base profile from the relation

$$\Lambda = \frac{16}{\pi}\int_0^1 \frac{y_t}{c}\sqrt{\left[1 - P_{f_i}\right]\left[1 + \left(\frac{dy_t}{dx}\right)^2\right]}\, d\left(\frac{x}{c}\right) \qquad (3)$$

where

y_t ordinate of base profile at chordwise station x

dy_t/dx slope of surface of base profile at x

P_{f_i} base-profile pressure coefficient at x in an incompressible fluid

(It will be noted that the quantity λt^2 in references 1 and 2 is equivalent to $\frac{1}{4}\Lambda c^2$ in the notation of this report.) Values of Λ for a number of base profiles are given in table I.

In appendix A, it is shown that the effect of compressibility upon the streamwise induced velocity at a given point a large distance above or below a body in a uniform stream is such as to multiply the velocity increment for incompressible flow by the factor $1/\left[1 - M^2\right]^{3/2}$ where M is the Mach number of the flow far upstream from the body. Applying this result to the velocity induced at the base profile by each of the airfoils in Lock's system of images, it can be seen that for a compressible fluid the increase in the effective axial velocity in the tunnel is

$$\Delta_1 V' = \frac{1}{\left[1 - (M')^2\right]^{3/2}}\Lambda\sigma V' \qquad (4)$$

where M' is the apparent Mach number - that is, the Mach number corresponding to the velocity V'.

It should be noted that equation (4) does not agree with the result given in reference 10, in which it is stated that the velocity increment in the incompressible fluid should be multiplied by the factor $1/\left[1 - (M')^2\right]$ to allow for the effect of fluid compressibility. A critical review of this latter report by

its author and by others has disclosed that the result given therein is incorrect. The error in the analysis arose from a failure to preserve the shape of the body for which the compressibility factor was being determined, so that the velocity at the surface of the body was influenced by a change in shape as well as by the tunnel-wall interference. This difficulty does not arise in the analysis of the present report. The result of equation (4) has also been obtained by an independent procedure in reference 5.

Consideration of the symmetry of the base profile and of the system of images used by Lock to simulate the effects of the tunnel walls indicates that the interaction between the walls and the base profile does not induce velocities normal to the center line of the tunnel. Similarly the base profile does not affect the longitudinal velocity gradient in the tunnel at the position of the airfoil.

Wake effect.- In the wake of an airfoil moving through a real fluid, the total head of the fluid is less than in the region outside the wake. This reduction arises from the increase in thermal energy caused by fluid friction in the boundary layer and in the wake itself and by any shock waves which may exist in the vicinity of the airfoil. Considering a section normal to the wake, it may be said that the static pressure across the stream is nearly constant if the section taken is not too close to the trailing edge of the airfoil. It follows that the reduction in total head which exists within the wake must appear almost entirely as a decrease in the local dynamic pressure of the fluid. This decrease arises primarily from a reduction in the local velocity and secondarily from the reduction in local density which accompanies the increased temperature within the wake. Thus, since the local velocity and density within the wake are both less than in the external flow, the mass-flow rate per unit area is less inside the wake than outside. This condition prevails both in the tunnel and in free air. In the tunnel, however, the requirement of continuity of flow between a transverse section upstream from the airfoil and a section across the wake necessitates, in addition, that the mass-flow rate per unit area outside of the wake is greater than the mass-flow rate per unit area ahead of the airfoil. In order to satisfy this requirement, the velocity in the tunnel outside of the wake must be greater than that of the undisturbed stream. This fact implies that as the flow proceeds down the tunnel the velocity of the main portion of the stream undergoes a gradual increase from the value prevailing in the undisturbed stream ahead of the model to some higher value downstream of the airfoil. This does not hold true in free air, where

the velocities of the main flow upstream and downstream of the model are equal. The interference between the wake and the tunnel walls thus gives rise at the position of the model to a velocity increment and a velocity gradient which are not present in an unlimited stream. Further, as required by Bernoulli's equation, the velocity gradient is accompanied by a longitudinal pressure gradient which likewise would not exist in free air.

To determine the magnitude of these effects the procedure is briefly as follows: Two stations in the tunnel are considered, one far upstream from the model and one far enough downstream so that the wake has spread to the walls and the velocity is again uniform across the tunnel. The difference in static pressure between these two stations is evaluated as a function of the measured drag of the airfoil. The pressure gradient at the airfoil can be related to this pressure difference and hence to the drag of the airfoil by a convenient analytic device, which is essentially the same as that used by Goldstein (reference 3). The airfoil and its wake are considered to be replaced by a fluid source located at the position of the airfoil. It is specified that conditions far upstream in the resulting hypothetical flow must be the same as those existing in the actual stream. With this provision, the magnitude of the velocity and static pressure far downstream can be determined as functions of the upstream conditions and the strength of the source. The strength is then related to the drag of the airfoil by requiring that the static pressure difference promoted between the two stations in the tunnel by the source flow is the same as that which actually exists when the airfoil and wake are present. The tunnel walls can then be replaced by an infinite system of such sources directly above and below the position of the airfoil at intervals equal to the height of the tunnel. The system of image sources alone, however, would induce a small finite negative velocity at infinity upstream, so that it is necessary to superpose on the flow field an additional uniform flow of equal velocity in the positive direction in order to satisfy the original requirement that the conditions far upstream shall be unchanged. The velocity of this flow, which is readily determined as a function of the source strength and hence of the airfoil drag, then gives the velocity increment caused at the airfoil by the interference between the wake and the walls. The longitudinal velocity and pressure gradients at the position of the airfoil are found in terms of the drag by evaluating the flow induced at that point by the image sources. It is apparent that this entire method of analysis fails to satisfy the actual condition as regards the velocity at infinity downstream. This discrepancy arises out of

the fundamental difference between the actual flow in the wake and the source flow by which it is represented and is unavoidable as long as this representation is used.

Consider the flow in a closed two-dimensional-flow wind tunnel, as shown in figure 1. At a station far upstream, the effect of the model upon the flow is negligible, so that the velocity V', the density ρ', the static pressure p', and the absolute temperature T' are constant across the stream. At a station far downstream, where the wake has spread to the walls, the velocity V'', the density ρ'', the pressure p'', and the absolute temperature T'' are again constant across the stream.

The difference between the pressures p' and p'' can be related to the measured drag of the airfoil by means of the conditions of continuity, conservation of energy, and impulse and momentum, together with the state relations for a perfect gas. The condition of continuity is given by

$$\rho' V' = \rho'' V'' \tag{5}$$

and, if it is assumed that the flow is an adiabatic process, conservation of total energy requires that

$$\frac{(V')^2}{2} - \frac{(V'')^2}{2} = gJc_p (T'' - T')$$

or

$$\frac{V''}{V'} = \left\{1 - \frac{2gJc_pT'}{(V')^2}\left(\frac{T''}{T'} - 1\right)\right\}^{1/2} \tag{6}$$

where

g gravitational acceleration

J mechanical equivalent of heat

c_p specific heat of gas at constant pressure

In modern wind tunnels the walls of the test section are flared slightly to compensate for the growth of the boundary layer on the walls, and only the drag of the airfoil therefore need be considered. The impulse-momentum equation can be written

$$\frac{D'}{h} = p' - p'' + \rho'(V')^2 - \rho''(V'')^2$$

or

$$\frac{1}{2} c_d' \left(\frac{c}{h}\right) = \frac{p' \left(1 - \frac{p''}{p'}\right)}{\rho'(V')^2} + 1 - \frac{\rho''}{\rho'} \left(\frac{V''}{V'}\right)^2 \tag{7}$$

where D' is the drag of the airfoil and c_d' the drag coefficient referred to the apparent dynamic pressure q'.

The velocity of sound V_c' in the undisturbed stream is related to the absolute temperature by

$$(V_c')^2 = \gamma R T' = (\gamma - 1) g J c_p T' \tag{8}$$

where γ is the ratio of specific heats and R is the gas constant. By means of this relation, equation (6) can be written

$$\frac{V''}{V'} = \left\{ 1 - \frac{2\left(\frac{T''}{T'} - 1\right)}{(\gamma - 1)(M')^2} \right\}^{1/2} \tag{9}$$

and, from equation (5),

$$\frac{\rho''}{\rho'} = \left\{ 1 - \frac{2\left(\frac{T''}{T'} - 1\right)}{(\gamma - 1)(M')^2} \right\}^{-1/2} \tag{10}$$

The state equation for a perfect gas then provides the relations

$$\frac{p''}{p'} = \frac{\rho'' T''}{\rho' T'} = \frac{T''}{T'} \left\{ 1 - \frac{2\left(\frac{T''}{T'} - 1\right)}{(\gamma - 1)(M')^2} \right\}^{-1/2} \tag{11}$$

and

$$\frac{p'}{\rho'(V')^2} = \frac{RT'}{(V')^2} = \frac{(V_c')^2}{\gamma (V')^2} = \frac{1}{\gamma (M')^2} \tag{12}$$

Substitution from equations (9), (10), (11), and (12) into equation (7) gives

$$\frac{1}{2} c_d' \left(\frac{c}{h}\right) = \frac{1}{\gamma(M')^2}\left\{\left[1 - \frac{T''}{T'}\left[1 - \frac{2\left(\frac{T''}{T'} - 1\right)}{(\gamma - 1)(M')^2}\right]^{-\frac{1}{2}}\right]\right\} + 1$$

$$- \left\{1 - \frac{2\left(\frac{T''}{T'} - 1\right)}{(\gamma - 1)(M')^2}\right\}^{1/2}$$

from which it can be found that

$$\left\{1 - \frac{2\left(\frac{T''}{T'} - 1\right)}{(\gamma - 1)(M')^2}\right\}^{\frac{1}{2}} = \frac{1 + \gamma(M')^2\left[1 - \frac{c_d'}{2}\left(\frac{c}{h}\right)\right]}{(\gamma + 1)(M')^2}$$

$$- \frac{\sqrt{\left[1 - (M')^2\right]^2 - \gamma(M')^2 \frac{c_d'}{2}\left(\frac{c}{h}\right)\left\{2 + \gamma(M')^2\left[2 - \frac{c_d'}{2}\left(\frac{c}{h}\right)\right]\right\}}}{(\gamma + 1)(M')^2} \quad (13)$$

For airfoils usually employed, the factor $c_d' \left(\frac{c}{h}\right)$ is small. Expanding the above expression and neglecting terms containing $c_d' \left(\frac{c}{h}\right)$ to powers higher than the first gives

$$\left\{1 - \frac{2\left(\frac{T''}{T'} - 1\right)}{(\gamma - 1)(M')^2}\right\}^{\frac{1}{2}} = 1 + \gamma \frac{c_d'}{2}\left(\frac{c}{h}\right)\frac{(M')^2}{1 - (M')^2} \quad (14)$$

By means of this relation, together with equations (9) and (10) the static pressure difference in terms of q' is obtained from equation (7) as

$$\frac{p' - p''}{q'} = c_d' \left(\frac{c}{h}\right)\left\{1 + \frac{\gamma(M')^2}{1 - (M')^2}\right\} \quad (15)$$

Now, consider the airfoil and wake to be removed and replaced by a fluid source of strength Q. If the flow conditions far upstream are maintained unchanged, the mass flow far downstream is then

$$h\rho_s''V_s'' = h\rho'V' + Q$$

or

$$\frac{\rho_s''V_s''}{\rho'V'} = 1 + \frac{Q}{h\rho'V'} \tag{16}$$

where the subscript s denotes conditions now prevailing at the latter station. For reversible adiabatic flow

$$\frac{\rho_s''}{\rho'} = \left\{1 - \frac{\gamma-1}{2}(M')^2\left[\left(\frac{V_s''}{V'}\right)^2 - 1\right]\right\}^{\frac{1}{\gamma-1}}$$

Since it is to be expected that (V_s''/V') will be close to unity, the right-hand side of this equation may be expanded in ascending powers of $\left[\left(\frac{V_s''}{V'}\right)^2 - 1\right]$, and terms containing powers higher than the first neglected. Thus,

$$\frac{\rho_s''}{\rho'} = 1 - \frac{(M')^2}{2}\left[\left(\frac{V_s''}{V'}\right)^2 - 1\right] \tag{17}$$

and equation (16) becomes

$$\frac{V_s''}{V'}\left\{1 - \frac{(M')^2}{2}\left[\left(\frac{V_s''}{V'}\right)^2 - 1\right]\right\} = 1 + \frac{Q}{h\rho'V'}$$

It is reasonable to assume that the ratio $\frac{Q}{h\rho'V'}$ is small as compared with unity. This solution of the preceding equation to the first order in $\frac{Q}{h\rho'V'}$ is

$$\left(\frac{V_s''}{V'}\right) = 1 + \frac{1}{1 - (M')^2} \frac{Q}{h\rho'V'} \tag{18}$$

Bernoulli's equation for reversible adiabatic flow can be written

$$\frac{p' - p_s''}{q'} = \frac{2}{\gamma(M')^2} \left[1 - \left\{ 1 - \frac{\gamma - 1}{2} (M')^2 \left[\left(\frac{V_s''}{V'} \right)^2 - 1 \right] \right\}^{\frac{\gamma}{\gamma - 1}} \right]$$

Since $\left(\frac{V_s''}{V'}\right)$ is close to unity, this may be replaced by the approximate relation

$$\frac{p' - p_s''}{q'} = \left(\frac{V_s''}{V'}\right)^2 - 1$$

Substitution from equation (18) and neglect of the term involving the square of $\frac{Q}{h\rho'V'}$ then gives

$$\frac{p' - p_s''}{q'} = \frac{2Q}{h\rho'V'} \frac{1}{1 - (M')^2} \tag{19}$$

Comparison of equations (15) and (19) shows that the source strength required to promote the same pressure difference as actually arises from the confinement of the airfoil wake is

$$Q = \frac{\rho'V'c_d'c}{2} \left\{ 1 - (\gamma - 1)(M')^2 \right\} \tag{20}$$

The tunnel walls are now replaced by an infinite system of sources of strength Q spaced h distance apart and located directly above and below the position of the airfoil as shown in figure 1. This image system together with the source which has been placed at the position of the airfoil satisfies the requirement that the flow at the plane of the tunnel wall shall be tangential to the wall.

As shown in the first of equations (A11) of appendix A, a source of strength Q in a uniform flow of compressible fluid will induce at a distance r from itself a streamwise velocity

$$\Delta V = \frac{Q}{2\pi\rho r}\left\{\frac{\cos\varphi}{\sqrt{1 - M^2}\,(1 - M^2\sin^2\varphi)}\right\}$$

where φ is the polar angle of the point in question and ρ and M are the density and Mach number of the undisturbed stream. By virtue of this relation, the streamwise velocity $\Delta_2 V'$ induced at a point of the center line of the tunnel by the entire system of image sources is

$$\Delta_2 V' = \sum_{m=1}^{\infty} \frac{Q}{\pi\rho' r_m}\left\{\frac{\cos\varphi_m}{\sqrt{1 - (M')^2}\,\left[1 - (M')^2\sin^2\varphi_m\right]}\right\}$$

where r_m and φ_m are the radial distance and the polar angle of the point relative to the source a distance mh above or below the center line and ρ' and M' are the density and Mach number of the undisturbed flow in the tunnel. If the distance from the position of the airfoil to the point on the center line is denoted by x (taken positive downstream), this equation can be written

$$\Delta_2 V' = \frac{Q}{\pi\rho'\sqrt{1 - (M')^2}} \sum_{m=1}^{\infty} \frac{x}{x^2 + \left[1 - (M')^2\right] m^2 h^2}$$

or

$$\Delta_2 V' = -\frac{Q}{\pi\rho'\sqrt{1-(M')^2}}\left[\frac{\pi}{2h\sqrt{1-(M')^2}}\coth\frac{\pi x}{h\sqrt{1-(M')^2}} - \frac{1}{2x}\right] \tag{21}$$

It can be seen by setting $x = -\infty$ in equation (21) that the image sources induce at an infinite distance upstream a velocity

$$(\Delta_2 V')_{-\infty} = -\frac{Q}{2\rho' h\left[1-(M')^2\right]}$$

In order to satisfy the original requirement that conditions far upstream remain unchanged, this velocity must be counterbalanced by the superposition of a uniform flow of equal magnitude but opposite sign. The addition of this flow at all points in the field will result in a speeding up of the general flow at the postiion of the airfoil by the amount

$$\Delta_3 V' = \frac{Q}{2\rho' h\left[1-(M')^2\right]}$$

or, substituting the source strength from equation (20),

$$\Delta_3 V' = \left\{\frac{1+(\gamma-1)(M')^2}{1-(M')^2}\right\}\frac{c_d'}{4}\left(\frac{c}{h}\right)V'$$

If the factor τ is defined as

$$\tau = \frac{1}{4}\left(\frac{c}{h}\right) \tag{22}$$

The velocity increment induced at the position of the airfoil by the interference between the wake and the walls may thus finally be written for air $(\gamma = 1.4)$ as

$$\Delta_3 V' = \frac{1+0.4(M')^2}{1-(M')^2}\tau c_d' V' \tag{23}$$

The longitudinal velocity gradient produced at the position of the airfoil by the flow from the image sources can be found by differentiating equation (21) with respect to x and then setting $x = 0$. This gives finally

$$\frac{dV'}{dx} = \frac{d(\Delta_2 V')}{dx} = \frac{\pi Q}{6\rho' h^2 \left[1 - (M')^2\right]^{3/2}}$$

or, by virtue of equation (20),

$$\frac{dV'}{dx} = \left\{\frac{1 + (\gamma - 1)(M')^2}{\left[1 - (M')^2\right]^{3/2}}\right\} \frac{\pi c_d' V' c}{12h^2} \tag{24}$$

It already has been noted that the interference associated with the thickness of the airfoil has no effect upon the longitudinal velocity gradient at the position of the airfoil. It will be seen later that this also is true of the interference associated with airfoil camber. Equation (24) thus gives the total velocity gradient for the complete airfoil and wake. The total pressure gradient at the position of the model then is given by Bernoulli's equation as

$$\frac{dp}{dx} = -\rho' V' \frac{dV'}{dx}$$

or, substituting from equation (24) and setting $\gamma = 1.4$,

$$\frac{dp}{dx} = -\left\{\frac{1 + 0.4(M')^2}{\left[1 - (M')^2\right]^{3/2}}\right\} \frac{\pi c_d' q' c}{6h^2} \tag{25}$$

It is apparent from the symmetry of the system of image sources that at the center line of the tunnel the interference between the wake and the walls has no effect upon the velocity normal to the direction of the stream.

It is shown later in this report that the camber of the airfoil does not affect the stream velocity at the airfoil. Equations

(4) and (23) together thus give the total increase in velocity for the complete airfoil and wake. The effective or true velocity V at the model is therefore

$$V = V'\left\{1 + \frac{1}{\left[1 - (M')^2\right]^{3/2}}\Delta\sigma + \frac{1 + 0.4(M')^2}{1 - (M')^2}\tau c_d'\right\} \tag{26}$$

It is evident that a correction to the apparent velocity in a compressible flow implies corrections also to the apparent density, dynamic pressure, Reynolds number, and Mach number. These corrections are readily obtained on the basis of the usual assumption that the flow is adiabatic. It is assumed that the correction terms are small as compared with unity, so that squares and products of these terms may be neglected.

The true density ρ at the model is connected with the apparent density ρ' by the insentropic relation

$$\rho = \rho'\left\{1 - \frac{\gamma - 1}{2}(M')^2\left[\left(\frac{V}{V'}\right)^2 - 1\right]\right\}^{\frac{1}{\gamma - 1}} \tag{27}$$

Substitution from equation (26) gives, after expansion as an ascending power series and neglect of correction terms higher than the first order,

$$\rho = \rho'\left\{1 - \frac{(M')^2}{\left[1 - (M')^2\right]^{3/2}}\Delta\sigma - \frac{(M')^2\left[1 + 0.4(M')^2\right]}{1 - (M')^2}\tau c_d'\right\} \tag{28}$$

The true dynamic pressure $q = \frac{1}{2}\rho V^2$ is related to the apparent dynamic pressure q' by the equation

$$q = q'\left(\frac{\rho}{\rho'}\right)\left(\frac{V}{V'}\right)^2$$

By means of equations (26) and (28) this can be written to the first order as

$$q = q' \left\{ 1 + \frac{2-(M')^2}{\left[1-(M')^2\right]^{3/2}} \Lambda\sigma + \frac{\left[2-(M')^2\right]\left[1+0.4(M')^2\right]}{1-(M')^2} \tau c_d' \right\} \qquad (29)$$

The true Reynolds number R is given in terms of the apparent Reynolds number R' by the equation

$$R = R' \left(\frac{\rho}{\rho'}\right)\left(\frac{\mu'}{\mu}\right)\left(\frac{V}{V'}\right)$$

where μ and μ' are the coefficients of viscosity corresponding to V and V'. According to Von Kármán and Tsien (reference 11), the coefficients of viscosity are related to the corresponding absolute temperatures by

$$\frac{\mu}{\mu'} = \left(\frac{T}{T'}\right)^{0.76}$$

For reversible adiabatic flow it can be shown that

$$T = T' \left\{ 1 - \frac{\gamma - 1}{2} (M')^2 \left[\left(\frac{V}{V'}\right)^2 - 1 \right] \right\} \qquad (30)$$

which after substitution from equation (26) becomes to the first order for air ($\gamma = 1.4$)

$$T=T' \left\{ 1 - \frac{0.4(M')^2}{\left[1-(M')^2\right]^{3/2}} \Lambda\sigma - \frac{0.4(M')^2\left[1+0.4(M')^2\right]}{1-(M')^2} \tau c_d' \right\} \qquad (31)$$

By means of these relations together with equations (26) and (28), the true Reynolds number may be written

$$R=R' \left\{ 1 + \frac{1-0.7(M')^2}{\left[1-(M')^2\right]^{3/2}} \Lambda\sigma + \frac{\left[1-0.7(M')^2\right]\left[1+0.4(M')^2\right]}{1-(M')^2} \tau c_d' \right\} \qquad (32)$$

The true Mach number M is related to the apparent Mach number M' by the equation

$$M = M' \left(\frac{V}{V'}\right)\left(\frac{V_c'}{V_c}\right)$$

where V_c and V_c' are the velocities of sound corresponding to V, and V'. Since the velocity of sound in a gas is directly proportional to the square root of the absolute temperature alone, this equation may also be written

$$M = M' \left(\frac{V}{V'}\right)\left(\frac{T'}{T}\right)^{1/2}$$

With the aid of equations (26) and (31) the true Mach number then may be written to the first order

$$M = M' \left\{ 1 + \frac{1+0.2(M')^2}{\left[1-(M')^2\right]^{3/2}} \Lambda\sigma + \frac{\left[1+0.2(M')^2\right]\left[1+0.4(M')^2\right]}{1-(M')^2} \tau c_d' \right\} \qquad (33)$$

At low Mach numbers, the terms containing $\tau c_d'$ in the correction equations are usually negligible as compared with the terms containing $\Lambda\sigma$. At supercritical Mach numbers, however, where the drag coefficient is very large, the terms with $\tau c_d'$ are predominant.

Numerical values of the compressibility factor appearing in equations (26), (29), (32), and (33) are given in table II.

Camber effect.- The theory of the infinitesimally thin, cambered airfoil in free air is developed by Glauert in reference 12 (pp. 87-93). In this development the camber line is replaced by a sheet of continuously distributed, bound vortices. The flow induced at any point on the camber line by this system of vortices is obtained by integration and is combined vectorially with the flow of the undisturbed stream to give the direction of the resultant flow. The distribution of vorticity is then determined from the condition that the resultant flow at all points on the camber line must be tangential to the camber line.

In the actual calculation of the induced velocity, it is assumed that the vortices may be distributed along the chord line rather than along the camber line and that the induced velocity at any chordwise station on the camber line is the same as the induced velocity on the chord line at the same station. If the origin of coordinates is taken at the leading edge of the airfoil (fig. 2), with the positive x-axis along the chord line and the positive y-axis directed upward, the induced velocity $(v)_i$ in an incompressible fluid at any point x_o on the chord line is

$$(v)_i = \frac{1}{2\pi}\int_0^c \frac{\frac{d\Gamma}{dx}\,dx}{x-x_o} \tag{34}$$

where $d\Gamma/dx$ is the vorticity per unit length at the point x and c is the chord of the airfoil. The direction of this velocity is normal to the x-axis.

Glauert (reference 7) has shown that a first approximation to the velocity induced at any point by a simple vortex in a compressible stream can be obtained by simply multiplying the velocity induced at the same point in an incompressible stream by the factor

$$\frac{\sqrt{1 - M^2}}{1 - M^2\sin^2\varphi} \tag{35}$$

where M is the Mach number of the undisturbed flow and φ the polar angle of the point in question as measured from the direction of flow of the undisturbed stream. For points on the chord of an airfoil which is inclined at a small angle to the direction of the undisturbed stream the polar angle φ is small, and the factor (35) is sensibly equal to

$$\sqrt{1 - M^2}$$

If it is assumed that the effect of a vortex sheet in a compressible fluid may be obtained by superposing the effects of elementary vortices, the velocity induced at any point x_o on the chord line in a compressible fluid is

$$v = \frac{\sqrt{1 - M^2}}{2\pi}\int \frac{\frac{d\Gamma}{dx}\,dx}{x - x_o} \tag{36}$$

If the undisturbed velocity of the free stream is taken equal to the true velocity V at the airfoil in the tunnel, the condition that the resultant flow shall be tangential to the camber line requires that, for all points on the airfoil,

$$\frac{v}{V} = \frac{dy_c}{dx} - \alpha \tag{37}$$

where dy_c/dx is the slope of the camber line at x_o and α is the true angle of attack; that is, the angle the undisturbed stream makes with the chord line in free air. (See fig. 2.)

The problem of the infinitesimally thin, cambered airfoil in a two-dimensional-flow tunnel can be investigated by the method of images; that is, the effect of the upper and lower walls of the tunnel can be simulated by introducing an infinite lattice of alternately inverted but otherwise identical image airfoils above and below the original airfoil, as shown in figure 3(a). By this artifice the direction of flow at the position of the upper and lower walls can be made to coincide with the plane of the walls, which is the required condition of flow. As in Glauert's analysis of the airfoil in free air, the camber line of the airfoil and of each of its images is replaced by a sheet of continuously distributed vortices, the vortex distribution of all sheets being identical in magnitude but alternately reversed in sign. The flow induced at any point of the camber line of the original airfoil by the entire vortex system is then obtained by integration. As before, the distribution of vorticity must be determined so that the resultant of the induced velocity and the stream velocity is tangential to the camber line of the airfoil.

For the detailed calculation, the coordinate system is taken as shown in figure 3(b). The origin of coordinates is taken on the center line of the tunnel at the leading edge of the airfoil. The positive x-axis extends downstream parallel to the undisturbed flow, and the positive y-axis is directed upwards. It is assumed that the vortices may be distributed along the x-axis and the induced velocities calculated at points on this axis. This arrangement is somewhat different from the system employed for the airfoil in free air, where the x-axis was taken along the chord line; however, since the angle of attack is assumed to be small, the difference is of no consequence.

It is evident from figure 3(b) that, for an airfoil midway between the upper and lower walls of the tunnel, the axial velocity induced at any point on the x-axis by any one image is nullified by the velocity induced by the corresponding image on the opposite side of the tunnel. It follows that airfoil camber does not affect either the true axial velocity or the longitudinal pressure gradient in the tunnel at the position of the model.

The vertical velocities induced at any point on the x-axis by any one image and its counterpart are, however, additive. Thus, for corresponding images situated at mh and $-mh$, respectively, the vertical velocity $(v'_{rm})_i$ induced at the point x_o in an incompressible fluid is

$$(v'_{rm})_i = 2\,(-1)^m \int_o^c \frac{\frac{d\Gamma'}{dx} \sin\left(\varphi_m - \frac{\pi}{2}\right) dx}{2\pi r_m}$$

or

$$(v'_{rm})_i = \frac{1}{\pi}\,(-1)^m \int_o^c \frac{\frac{d\Gamma'}{dx}\,(x - x_o)\,dx}{(x - x_o)^2 + (mh)^2} \tag{38}$$

where $d\Gamma'/dx$ is the vorticity per unit length at the point x in the tunnel.

It will now be assumed that the chord of the airfoil is reasonably small in comparison with the height of the tunnel. This being the case, the approximation

$$(x - x_o)^2 + (mh)^2 \cong (mh)^2$$

is sufficiently precise for purposes of this analysis, and the term $(x - x_o)^2$ in the denominator of equation (38) may be neglected.

The vertical velocity $(v'_r)_i$ induced by all the images is then found by superposition as

$$(v'_r)_i = \frac{1}{\pi h^2} \sum_{m=1}^{\infty} \frac{(-1)^m}{m^2} \int_o^c (x - x_o) \frac{d\Gamma'}{dx}\,dx$$

$$= -\frac{\pi}{12h^2}\int_0^c (x - x_o)\frac{d\Gamma'}{dx}\,dx \qquad (39)$$

This equation can be corrected for the effect of compressibility by means of expression (35). If, as was assumed, the chord of the airfoil is reasonably small as compared with the tunnel height, the polar angle φ of any point x_o on the airfoil with respect to any point x on an image is nearly a right angle, so that in this case the factor (35) is sensibly equal to

$$\frac{1}{\sqrt{1 - M^2}}$$

The vertical velocity induced in a compressible stream by all the images is then

$$v'_r = -\frac{\pi}{12h^2\sqrt{1 - M^2}}\int_0^c (x - x_o)\frac{d\Gamma'}{dx}\,dx \qquad (40)$$

The vertical velocity v'_b, induced at a point x_o by the vortex sheet belonging to the airfoil itself, is given by equation (36) if Γ' and v'_b are substituted for Γ and v, respectively.

The total vertical induced velocity v' at any point x_o on the airfoil in the tunnel is then the sum of v'_r and v'_b; that is,

$$v' = \frac{\sqrt{1 - M^2}}{2\pi}\int_0^c \left[\frac{1}{x - x_o} - \frac{\pi^2}{6h^2(1 - M^2)}(x - x_o)\right]\frac{d\Gamma'}{dx}\,dx \qquad (41)$$

The condition that the resultant of the induced velocity and the true axial velocity at the airfoil shall be tangential to the camber line requires that, at all points on the camber line,

$$\frac{v'}{V} = \frac{dy_c}{dx} - \alpha' \qquad (42)$$

where α' is the angle of attack of the airfoil in the tunnel; that is, the angle the chord line makes with the center line of the tunnel. The true velocity V rather than the apparent velocity V' is used in equation (42), since the vortex system used to represent the cambered airfoil in the tunnel is actually operating in a stream of velocity V when the airfoil thickness and wake are present.

Relations between Characteristics of Airfoil in Tunnel and in Free Air

The preceding sections provide the basic information required for the development of relations between the characteristics of the airfoil in the tunnel and in free air. The relations for the lift and moment coefficients and angle of attack are derived from the equations of the preceding section by an extension of the method of Fourier series employed in Glauert's theory of thin airfoils (reference 12, pp. 87-93). To this end, the vorticity distributions for the airfoil in the tunnel and in free air are each represented by a trigonometric series, the two series being similar in form but having undetermined coefficients. By means of the equations of the preceding section, general relations are found between the coefficients of the two series. These general relations are then specialized to meet the requirement that the airfoil shall have the same value of the cotangent term of the series in the tunnel and in free air, this requirement being shown to be necessary to assure that the essential characteristics of the pressure distribution will be sensibly the same in both cases. By means of the relations between the coefficients, expressions are then derived for the lift and moment coefficients and angle of attack of the airfoil in free air in terms of the characteristics measured in the tunnel. The corresponding drag coefficient in free air can be found from the drag measured in the tunnel by subtracting the pressure drag caused by the interference between the walls and the wake and referring the remaining drag to the true instead of the apparent dynamic pressure. Finally, a method is presented for correcting airfoil pressure distributions for the effect of tunnel walls.

To carry out the analysis, points on the airfoil are defined by a new coordinate θ such that

$$x = \frac{1}{2} c (1 - \cos \theta) \qquad (43)$$

and

$$dx = \frac{1}{2} c \sin\theta \, d\theta \tag{44}$$

The distribution of vorticity along the chord of the airfoil in free air is represented, after Glauert, by the trigonometric series

$$\frac{d\Gamma}{dx} = 2V \left\{ A_0 \cot\frac{1}{2}\theta + \sum_{n=1}^{\infty} A_n \sin n\theta \right\} \tag{45}$$

Equation (36) then gives the induced velocity at any point θ on the airfoil as

$$\frac{v}{V} = \sqrt{1 - M^2} \left\{ -A_0 + \sum_{n=1}^{\infty} A_n \cos n\theta \right\}$$

and equation (37) for the slope of the mean-camber line becomes

$$\frac{dy_c}{dx} = \alpha - \sqrt{1 - M^2}\, A_0 + \sqrt{1 - M^2} \sum_{n=1}^{\infty} A_n \cos n\theta \tag{46}$$

The coefficients are then given by the relations

$$\left.\begin{aligned} \alpha - \sqrt{1 - M^2}\, A_0 &= \int_0^{\pi} \frac{dy_c}{dx} \, d\theta \\ A_n &= \frac{1}{\sqrt{1 - M^2}} \frac{2}{\pi} \int_0^{\pi} \frac{dy_c}{dx} \cos n\theta \, d\theta \end{aligned}\right\} \tag{47}$$

For the airfoil in free air the coefficients A_n for $n \geq 1$ are thus functions of the camber-line shape only and are independent of the angle of attack. The coefficient A_0 is a function of both the camber-line shape and the angle of attack.

The chordwise lift distribution in free air is given by

$$\frac{dL}{dx} = \rho V \frac{d\Gamma}{dx} = q \frac{2}{V} \frac{d\Gamma}{dx}$$

which after substitution from equation (45) can be written in coefficient form as

$$P = \frac{1}{q} \frac{dL}{dx} = 4 \left\{ A_0 \cot \frac{1}{2} \theta + \sum_{n=1}^{\infty} A_n \sin n\theta \right\} \tag{48}$$

Equation (48) illustrates the well-known fact that in free air the chordwise lift distribution consists essentially of two distinct parts. The one part, contributed by the sine terms and generally referred to as the basic lift distribution (reference 13), depends in magnitude and form only upon the shape of the mean-camber line. The other part, defined by the cotangent term and referred to as the additional lift distribution, is fixed in form and depends in magnitude upon the angle of attack as well as upon the camber-line shape.

The distribution of vorticity for the airfoil in the tunnel is represented by

$$\frac{d\Gamma'}{dx} = 2V \left\{ A_0' \cot \frac{1}{2} \theta + \sum_{n=1}^{\infty} A_n' \sin n\theta \right\} \tag{49}$$

Substitution of this expression, together with expressions (43) and (44), into equation (41) gives, after integration,

$$\frac{v'}{V} = \sqrt{1 - M^2} \left\{ - A_0' + \frac{\sigma}{1 - M^2} \left(A_0' + \frac{1}{2} A_2' \right) + \left[A_1' - \frac{\sigma}{1 - M^2} (2A_0' + A_1') \right] \cos \theta + \sum_{n=2}^{\infty} A_n' \cos n\theta \right\}$$

where σ is as defined by equation (2). Equation (42) for the slope of the mean-camber line thus becomes

$$\frac{dy_c}{dx} = \alpha' - \sqrt{1 - M^2}\left[A_0' - \frac{\sigma}{1 - M^2}\left(A_0' + \frac{1}{2}A_2'\right)\right] + \sqrt{1 - M^2}\left[A_1' - \frac{\sigma}{1 - M^2}(2A_0' + A_1')\right]\cos\theta + \sqrt{1 - M^2}\sum_{n=2}^{\infty} A_n' \cos n\theta \tag{50}$$

The coefficients in this case are given by the relations

$$\left.\begin{aligned} \alpha' - \sqrt{1 - M^2}\left[A_0' - \frac{\sigma}{1 - M^2}\left(A_0' + \frac{1}{2}A_2'\right)\right] &= \int_0^{\pi} \frac{dy_c}{dx}\, d\theta \\ A_1' - \frac{\sigma}{1 - M^2}(2A_0' + A_1') &= \frac{1}{\sqrt{1 - M^2}}\frac{2}{\pi}\int_0^{\pi} \frac{dy_c}{dx}\cos\theta\, d\theta \\ A_n' &= \frac{1}{\sqrt{1 - M^2}}\frac{2}{\pi}\int_0^{\pi} \frac{dy_c}{dx}\cos n\theta\, d\theta, \quad n \geq 2 \end{aligned}\right\} \tag{51}$$

Thus for the airfoil in the tunnel the coefficient A_0' is a function of both the angle of attack and the shape of the camber line, but the functional relationship is altered from what it was in free air by the inclusion of terms proportional to σ. Furthermore, because of the appearance of the term involving A_0' in the second of equations (51), the coefficient A_1' is in this case also a function of the angle of attack, as well as of the camber-line shape. Since A_0' appears in this equation multiplied by the factor σ, the dependence upon the angle of attack is, however, secondary as compared with the dependence upon the shape of

the camber line. As in the case of the airfoil in free air, the coefficients A_n' for $n \geq 2$ are functions of the camber-line shape only.

The chordwise lift distribution in the tunnel is given by

$$\frac{dL'}{dx} = \rho V \frac{d\Gamma'}{dx} = q \frac{2}{V} \frac{d\Gamma'}{dx}$$

or in coefficient form,

$$P^* = \frac{1}{q} \frac{dL'}{dx} = 4 \left\{ A_0' \cot \frac{1}{2} \theta + \sum_{n=1}^{\infty} A_n' \sin n\theta \right\} \qquad (52)$$

In writing this equation the streamwise velocity gradient which results from the wall-wake interference (equation (24)) is ignored. It can be shown that the inclusion of this variable would give rise to correction terms of the order $\sigma c_d'$. Terms of this order are usually small as compared with the terms of order σ and $\tau c_d'$ considered in the theory and may therefore be neglected.

It is apparent from equation (52) that, as in the case of the airfoil in free air, the lift distribution in the tunnel may be divided into two components. Now, however, the component which depends upon the angle of attach includes both the cotangent term and the first sine term. The component which is a function of the camber-line shape alone, comprises the sine terms corresponding to $n \geq 2$. Again, these two components could be denoted by the terms "additional" and "basic" in the sense previously employed; however, since the phrase "additional lift" already is so firmly established with reference to the distinctive cotangent term alone, this usage does not appear advisable in the present case. For this reason, the terms of the series will be referred to by reference to their form or their position in the series.

Since it is the same airfoil which is being considered in both cases, equations (47) and (51) lead to the following general relations between the coefficients in free air and in the tunnel:

$$\left.\begin{aligned}
&\alpha - \sqrt{1 - M^2}\, A_0 = \alpha' - \sqrt{1 - M^2}\, A_0' + \frac{\sigma}{\sqrt{1 - M^2}}\left(A_0' + \frac{1}{2} A_2'\right) \\
&A_1 = A_1' - \frac{\sigma}{1 - M^2}\,(2A_0' + A_1') \\
&A_2 = A_2' \\
&- - - - - \\
&A_n = A_n'
\end{aligned}\right\} \quad (53)$$

In order to use these expressions to relate the characteristics of the airfoil in free air with those in the tunnel, it is necessary to choose some quantity or condition which will be maintained the same in both cases and relate the remaining quantities in accordance with this choice. If it were possible, the ideal procedure would be to keep all the aerodynamic coefficients unaltered and to determine a corresponding relationship between the angle of attack in the tunnel and in free air. To do this it would be necessary to keep all pressure and frictional forces the same in both cases, which can be accomplished only if the pressure distributions are identical. This would require that each of the coefficients A_n in equation (48) be equal to the corresponding coefficient A_n' in equation (52). It is apparent from the second of equations (53), however, that this requirement cannot, in general, be satisfied.

Although the pressure distribution cannot be maintained completely unaltered in the transfer from the tunnel to free air, the general relations (53) can be specialized in such a way that the essential character of the distribution is unchanged. It is apparent that the component of lift contributed by the first, or cotangent, term in equations (48) and (52) is different in form from that contributed by the series of sine terms. The cotangent component has an infinite value at the leading edge ($\theta = 0$) and a relatively large chordwise gradient of lift over most of the chord of the airfoil. The sine-series component is finite at all points and, for airfoils ordinarily encountered in practice, has a relatively small chordwise gradient, except possibly in the immediate

vicinity of the leading or trailing edges. The cotangent component with its infinite peak pertains, of course, only to the hypothetical airfoil of infinitesimal thickness and zero leading-edge radius. For all real airfoils, the lift at the leading edge can never be infinite; however, even in this instance the lift distribution is characterized by a component the form of which is peaked near the leading edge and the magnitude of which varies markedly with the angle of attack. The magnitude of this component is a primary factor in determining the character of the pressure distribution, and even a relatively small change in magnitude may cause considerable change in the minimum pressure and in the chordwise pressure gradients attained on the surface of the airfoil. Further, the aerodynamic characteristics which depend upon these quantities, particularly the profile drag, maximum lift, and critical compressibility speed, will be correspondingly altered. It follows that properly to correct airfoil data obtained in a wind tunnel to conditions in free air, the corrected quantities should correspond to the same magnitude of the peaked lift component as exists on the airfoil in the tunnel.

The requirement that the peaked component of lift on the real airfoil shall be the same in the tunnel and in free air can be expressed with reference to the assumed airfoil of infinitesimal thickness and camber by setting A_0 equal to A_0' in equations (53). The first of these equations, which relates the angle of attack in the two conditions, then becomes

$$\alpha = \alpha' + \frac{\sigma}{\sqrt{1 - M^2}} \left(A_0' + \frac{1}{2} A_2' \right) \tag{54}$$

and the relations between the coefficients are

$$\left.\begin{aligned} A_0 &= A_0' \\ A_1 &= A_1' - \frac{\sigma}{1 - M^2} (2A_0' + A_1') \\ A_2 &= A_2' \\ &- - - - \\ A_n &= A_n' \end{aligned}\right\} \tag{55}$$

Substitution from equations (55) into equation (48) gives

$$P = 4\left\{A_0' \cot\frac{1}{2}\theta - \frac{\sigma}{1-M^2}(2A_0' + A_1')\sin\theta + \sum_{n=1}^{\infty} A_n' \sin n\theta\right\}$$

or

$$P = P^* - \frac{4\sigma}{1 - M^2}(2A_0' + A_1')\sin\theta \qquad (56)$$

Thus, if the angle of attack in the tunnel and the angle of attack in free air are such as to satisfy equation (54), the chordwise lift distributions will differ by an amount defined by the second term on the right-hand side of equation (56).

The lift coefficient for the airfoil in free air is

$$c_l = \int_0^1 P\, d\left(\frac{x}{c}\right)$$

which, after substitution from equations (44) and (48), can be integrated to give

$$c_l = \pi(2A_0 + A_1) \qquad (57)$$

The quarter-chord-moment coefficient is

$$c_{m_{\frac{c}{4}}} = \int_0^1 P\left(\frac{1}{4} - \frac{x}{c}\right) d\left(\frac{x}{c}\right)$$

which becomes after integration

$$c_{m_{\frac{c}{4}}} = -\frac{\pi}{4}(A_1 - A_2) \qquad (58)$$

In usual wind-tunnel practice, the measured coefficients are referred to the apparent dynamic pressure q'. The lift distribution over the airfoil in the tunnel in terms of q' is

$$P' = \frac{1}{q'}\frac{dL'}{dx} = \frac{2}{V}\frac{q}{q'}\frac{d\Gamma}{dx}$$

Substitution from equation (49) gives

$$P' = 4\frac{q}{q'}\left\{A_0' \cot\frac{1}{2}\theta + \sum_{n=1}^{\infty} A_n' \sin n\theta\right\} \tag{59}$$

The lift and moment coefficients of the airfoil in the tunnel as referred to the apparent dynamic pressure are then, respectively,

$$c_l' = \int_0^1 P' d\left(\frac{x}{c}\right) = \pi\frac{q}{q'}(2A_0' + A_1') \tag{60}$$

and

$$c_{m_{\frac{c}{4}}}' = \int_0^1 P'\left(\frac{1}{4} - \frac{x}{c}\right) d\left(\frac{x}{c}\right) = -\frac{\pi}{4}\frac{q}{q'}(A_1' - A_2') \tag{61}$$

Relations between the coefficients in free air and in the tunnel can now be found with the aid of equations (55). Substitution of values from these equations into equation (57) gives

$$c_l = \pi(2A_0' + A_1')\left(1 - \frac{\sigma}{1 - M^2}\right)$$

$$= c_l'\frac{q'}{q}\left(1 - \frac{\sigma}{1 - M^2}\right)$$

Substitution from equation (29) and neglect of correction terms of higher than the first order then give

$$c_l = c_l'\left\{1 - \frac{\sigma}{1-M^2} - \frac{2 - (M')^2}{\left[1-(M')^2\right]^{3/2}}\Lambda\sigma - \frac{\left[2-(M')^2\right]\left[1+0.4(M')^2\right]}{1 - (M')^2}\tau c_d'\right\}$$

From equation (33) it can be seen that, to the first order, M may be replaced by M' in this equation. The final equation for the correction of the measured lift coefficient is therefore

$$c_l = c_l'\left\{1 - \frac{\sigma}{1 - (M')^2} - \frac{2 - (M')^2}{\left[1 - (M')^2\right]^{3/2}}\Lambda\sigma - \frac{\left[2 - (M')^2\right]\left[1 + 0.4(M')^2\right]}{1 - (M')^2}\tau c_d'\right\} \tag{62}$$

Similarly, substitution of values from equations (55) into equation (58) gives

$$c_{m_{\frac{c}{4}}} = -\frac{\pi}{4}(A_1' - A_2') + \frac{\pi}{4}(2A_0' + A_1')\frac{\sigma}{1 - M^2}$$

$$= \frac{q'}{q} c_{m_{\frac{c}{4}}}' + \frac{1}{4} c_l' \frac{\sigma}{1 - M^2}$$

To the order of approximation previously employed, the final equation for the correction of the measured moment coefficient can be written

$$c_{m_{\frac{c}{4}}} = c_{m_{\frac{c}{4}}}' \left\{ 1 - \frac{2-(M')^2}{\left[1-(M')^2\right]^{5/2}} \Lambda\sigma - \frac{\left[2-(M')^2\right]\left[1+0.4(M')^2\right]}{1-(M')^2} \tau c_d' \right\}$$

$$+ c_l' \frac{\sigma}{4\left[1-(M')^2\right]} \tag{63}$$

The corresponding angle of attack in free air can be found from equation (54). Combination of equations (60) and (61) gives

$$A_0' + \frac{1}{2} A_2' = \frac{q'}{q} \left\{ \frac{c_l' + 4c_{m_{\frac{c}{4}}}'}{2\pi} \right\}$$

To the first order, equation (54) then gives for the corrected angle of attack in radian measure

$$\alpha = \alpha' + \frac{\sigma}{2\pi\sqrt{1 - (M')^2}} \left\{ c_l' + 4c_{m_{\frac{c}{4}}}' \right\} \tag{64a}$$

or in degrees

$$\alpha = \alpha' + \frac{57.3\sigma}{2\pi\sqrt{1 - (M')^2}} \left\{ c_l' + 4c_{m_{\frac{c}{4}}}' \right\} \tag{64b}$$

Numerical values of the compressibility factors appearing in equations (62), (63), and (64) are given in table II.

It should not be implied from equations (64) that the general inclination of the stream at the position of the airfoil in the tunnel is actually different from what it would be if the walls were not present. The equations indicate rather that, with regard to the magnitude of the cotangent component of lift distribution, an airfoil at a given angle of attack in the tunnel behaves as though it were at a different angle in free air. This difference occurs because the tunnel walls give rise effectively to a change in the curvature of the stream at the position of the airfoil.

As was indicated previously, the essential character of the pressure distribution over a given airfoil will be the same in the tunnel and in free air, provided the magnitude of the cotangent lift component is the same in both cases; that is, provided the angles of attack are such as to satisfy equations (64). The exact shape of the pressure distributions, however, will still differ slightly for two reasons: (a) The interference between the lift and the tunnel walls causes a difference in chordwise lift distribution as required by equation (56), and (b) the interference between the wake and the walls gives rise to a longitudinal pressure gradient defined by equation (25). The effect of these two influences upon the remaining airfoil characteristics, the profile-drag coefficient, must be considered.

As given by equation (56), the chordwise lift distributions in the tunnel and in free air differ by an amount

$$\Delta P = P^* - P = \frac{4\sigma}{1 - M^2} (2A_c' + A_1') \sin\theta$$

which, by virtue of equation (60), may be written to the first order as

$$\Delta P = \frac{4}{\pi} \frac{\sigma}{1 - M^2} c_l' \sin\theta \qquad (65)$$

The changes in peak pressure and pressure gradient brought about by this increment of lift distribution, unlike the changes which would accompany even a minor alteration of the cotangent lift component, are ordinarily small. At low Mach numbers the drag depends primarily upon the character of the flow in the boundary layer, and, since this flow will not ordinarily be altered greatly by these small changes in the pressure distribution, the increment of lift distribution should have only a small effect upon the

profile drag. At high Mach numbers the drag is determined primarily by the total-head losses in the shock waves which appear after the critical Mach number is reached; that is, after the local speed of sound is obtained at the minimum pressure point on the airfoil. The critical Mach number is usually reduced by the change in peak pressure accompanying the change ΔP in lift distribution, but it can be shown that this reduction is ordinarily very small. It is reasonable to expect that the change in profile drag at a given supercritical Mach number is correspondingly small. These changes are discussed in further detail later in the report, but for the present it may be assumed that the difference in chordwise lift distribution between the tunnel and free air has only a negligible effect upon the profile drag.

For usual airfoils and drag coefficients, the longitudinal pressure gradient defined by equation (25) is also small, and its effect upon the boundary-layer flow and hence upon the frictional drag of the airfoil may be neglected. It will, however, increase the pressure drag by an amount which is comparable to differences already retained in the corrections to the lift and moment. This increase in pressure drag must be subtracted from the drag measured in the tunnel to obtain the true profile drag of the airfoil in free air.

Glauert has shown (reference 2, pp. 62-63) that in an incompressible fluid the drag experienced by an airfoil as the result of a streamwise pressure gradient is, in the notation of this paper,

$$\Delta D = -\frac{\pi}{8} \Lambda c^2 \frac{dp}{dx} = -\frac{6h^2}{\pi} \Lambda\sigma \frac{dp}{dx} \tag{66}$$

In appendix A, it is shown that this relation is unchanged by the effect of fluid compressibility. Substitution of dp/dx from equation (25) then gives for the drag due to the interference between the wake and the walls

$$\Delta D = c_d' \, q' \, c \left\{ \frac{1 + 0.4(M')^2}{\left[1 - (M')^2\right]^{3/2}} \right\} \Lambda\sigma$$

The true profile drag of the airfoil in free air is then

$$D = D' - \Delta D$$

$$= c_d' \, q' \, c \left\{ 1 - \frac{1 + 0.4(M')^2}{\left[1 - (M')^2\right]^{3/2}} \Lambda\sigma \right\}$$

and the corresponding drag coefficient referred to the true dynamic pressure is

$$c_d = \frac{D}{qc} = c_d' \left(\frac{q'}{q}\right) \left\{1 - \frac{1 + 0.4(M')^2}{\left[1 - (M')^2\right]^{3/2}} \Lambda\sigma\right\}$$

Substitution from equation (29) gives for the final correction to the measured drag coefficient

$$c_d = c_d' \left\{1 - \frac{2 - (M')^2}{\left[1 - (M')^2\right]^{3/2}} \Lambda\sigma - \frac{1 + 0.4(M')^2}{\left[1 - (M')^2\right]^{3/2}} \Lambda\sigma - \frac{\left[2 - (M')^2\right]\left[1 + 0.4(M')^2\right]}{1 - (M')^2} \tau c_d'\right\} \qquad (67)$$

It will be noted that, of the two correction terms involving $\Lambda\sigma$ in this equation, the first appears as a result of the change in dynamic pressure occasioned by the interference between the walls and the airfoil thickness; the second represents the effect of the pressure gradient induced by the interference between the walls and the wake. The correction term containing $\tau c_d'$ appears as a result of the change in dynamic pressure caused by the wall-wake interference. Numerical values of the functions of M' which appear in equation (67) are given in table II. The corrected drag coefficient corresponds, of course, to the corrected lift and moment coefficients as given by equations (62) and (63) and to the corrected angle of attack as given by equation (64a) or (64b).

The drag correction of equation (67) was determined particularly for drags measured with a balance and, as derived, is not necessarily correct for drags measured by the wake-survey method. It can be shown, however, from theoretical considerations of momentum and continuity in a two-dimensional-flow tunnel that for normal ratios of airfoil chord to tunnel height, the ordinary type of wake survey derived for free-air conditions gives, when applied in the tunnel, a value of the drag equal to that measured by the balance except for a negligible difference of less than one-half of one percent. Equation (67) may thus also be used to correct drag coefficients determined by the wake-survey method.

It should be noted that no correction to the drag has been made for any pressure gradient which may exist inherently in the

tunnel as a result of the streamwise growth of the boundary layer on the tunnel walls. Most modern tunnels are constructed so that this pressure gradient is sensibly zero; however, if such a gradient does exist and its magnitude is known, an approximate correction to the airfoil drag can be made by means of equation (66).

There remains the necessity for correcting the measured pressure distribution over the surface of the airfoil. The pressure at any point on the airfoil is conveniently expressed by the pressure coefficient S_l defined by

$$S_l = \frac{H - p_l}{q} \tag{68}$$

or by the pressure coefficient P_l defined by

$$P_l = \frac{p_l - p}{q} \tag{69}$$

where p_l is the local static pressure on the surface of the airfoil and H, p, and q are, respectively, the total head, static pressure, and dynamic pressure of the undisturbed stream. As indicated in reference 14, in a compressible stream,

$$H = p + q\,(1 + \eta) \tag{70}$$

where $(1 + \eta)$ for air $(\gamma = 1.4)$ is defined by the series

$$1 + \eta = 1 + \frac{M^2}{4} + \frac{M^4}{40} + \frac{M^6}{1600} + \cdots \tag{71}$$

M being the Mach number of the stream. From these relations it is readily shown that

$$S_l = (1 + \eta) - P_l \tag{72}$$

A curve of $(1 + \eta)$ versus M, as calculated from equation (71), is given in figure 4.

In reference 6 a method is presented for the determination of the pressure distribution around an airfoil in an incompressible stream when the lift distribution along the chord and the

pressure distribution over the base profile are known. The upper- and lower-surface pressures at any chordwise station x are given in coefficient form by

$$\left.\begin{aligned} P_U &= \frac{p_U - p}{q} = 1 - \frac{\left[(1 - P_f) + \frac{1}{4} P\right]^2}{(1 - P_f)} \\ P_L &= \frac{p_L - p}{q} = 1 - \frac{\left[(1 - P_f) - \frac{1}{4} P\right]^2}{(1 - P_f)} \end{aligned}\right\} \qquad (73)$$

where P_f is the pressure coefficient on the base profile at x, and P is the coefficient of lift per unit of chord at x. By following the basic reasoning of reference 6 and assuming that the induced velocities at the surface of the airfoil are small as compared with the velocity of the undisturbed stream, it is readily shown that equations (73) may also be applied to the pressure distribution in a compressible stream. In such application, the values of P_U, P_L, P_f, and P must all correspond, of course, to the same free-stream Mach number.

The measured pressure distribution is now readily corrected for the effect of the tunnel walls. It is only necessary to refer the measured pressure coefficients to the true instead of the apparent dynamic pressure and remove the effect of the lift distribution represented by equation (65). Strictly speaking, correction should also be made for the pressure gradient due to the wall-wake interference; however, in practical tests such correction is small and may be neglected. The detailed procedure is then as follows:

(1) The apparent upper- and lower-surface pressure coefficients

$$S_U' = \frac{H - p_U'}{q'} \quad \text{and} \quad S_L' = \frac{H - p_L'}{q'}$$

are obtained from the experimental results for the various chordwise stations.

(2) These pressure coefficients are referred to the true dynamic pressure by means of the equations

$$\left.\begin{aligned} S_U^* = S_U'\left(\frac{q'}{q}\right) = S_U'\left\{1 - \frac{2-(M')^2}{\left[1-(M')^2\right]^{3/2}}\Lambda\sigma - \frac{\left[2-(M')^2\right]\left[1+0.4(M')^2\right]}{1-(M')^2}\tau c_d'\right\} \\ S_L^* = S_L'\left(\frac{q'}{q}\right) = S_L'\left\{1 - \frac{2-(M')^2}{\left[1-(M')^2\right]^{3/2}}\Lambda\sigma - \frac{\left[2-(M')^2\right]\left[1+0.4(M')^2\right]}{1-(M')^2}\tau c_d'\right\} \end{aligned}\right\} \quad (74)$$

(3) The quantities $(1 - P_U^*)$ and $(1 - P_L^*)$ are determined in accordance with equation (72) as

$$\begin{aligned} 1 - P_U^* &= S_U^* - \eta \\ 1 - P_L^* &= S_L^* - \eta \end{aligned} \quad (75)$$

where η is determined by figure 4 for the true Mach number as given by equation (33).

(4) The chordwise lift distribution in the tunnel is found from

$$P^* = \frac{p_L' - p_U'}{q} = S_U^* - S_L^* \quad (76)$$

(5) The chordwise lift distribution in free air is determined from equation (65), which may be written

$$P = P^* - \frac{\sigma}{1 - (M')^2} P_e c_l' \quad (77)$$

where P_e is given by

$$P_e = \frac{4}{\pi}\sin\theta = \frac{4}{\pi}\sqrt{1 - \left(1 - \frac{2x}{c}\right)^2} \quad (78)$$

This quantity, which is termed the "interference lift distribution," is seen to be elliptic in form. Values of P_e at standard chordwise stations are given in table III.

(6) The quantity $(1 - P_f)$, where P_f is the base-profile pressure coefficient in free air, is given by the equation

$$(1 - P_f) = (1 - P_f^*) = \left(\frac{\sqrt{1 - P_U^*} + \sqrt{1 - P_L^*}}{2} \right)^2 \qquad (79)$$

which is obtained by combing equations (73).

(7) The values of P and $(1 - P_f)$ being known, the upper- and lower-surface pressure coefficients P_U and P_L are determined from equations (73). If desired, the corresponding coefficients S_U and S_L can be found from equation (72).

The corrected pressure distribution obtained by this method corresponds to the corrected angle of attack as given by equation (64a) or (64b) and to the corrected lift and moment coefficients as given by equations (62) and (63).

It has been mentioned previously that the correction to the angle of attack appearing in equations (64) does not represent an actual rotation of the stream direction. This fact is implicit in the derivation of the equations, but it can also be demonstrated by simple considerations of force and momentum. For this purpose it is sufficient to consider a simple incompressible potential flow in the tunnel and ignore the effect of the profile drag. Assume for the time being that, because of the interference between the airfoil and the tunnel walls, the general direction of the stream at the airfoil is inclined from its original direction parallel to the tunnel walls. For potential flow the resultant force acting on the airfoil must be at right angles to the local direction of the stream. The airfoil thus would be acted upon under the assumed conditions by a component of force parallel to the center line of the tunnel and would in reaction exert an equal and opposite force on the flow. Since the tunnel walls cannot in a potential flow exert a force parallel to the center line, this longitudinal force would have to be balanced by a difference of pressure or momentum between two stations in the tunnel, one upstream and one downstream from the airfoil. If the stations are taken far enough from the airfoil that its induced velocities are negligible, conditions across the tunnel are uniform at each station. It then follows from considerations of continuity of the incompressible flow in the tunnel that the conditions at the two stations are identical, and no difference

of pressure or momentum is possible. Thus the original assumption of a general rotation of the stream direction at the position of the airfoil is untenable. This conclusion is not changed by the effects of fluid compressibility. Furthermore, the fact that the introduction of the profile drag and the accompanying wake causes a pressure difference between the two stations likewise does not alter the result, as the wake effects are considered in the theory to be superposed on the potential-flow field. Thus, the angle correction appearing in equations (64) must be due to some cause other than a general inclination of the stream. As previously pointed out, it is actually due to an effective change in the curvature of the stream at the position of the airfoil and is a direct consequence of the requirement that the airfoil in this stream shall have the same cotangent component of lift distribution as does the airfoil in free air. These considerations are important in the proper interpretation of drag measurements from a two-dimensional-flow tunnel.

In the development of the correction to the measured drag coefficient, it was assumed that the increment ΔP in chordwise lift distribution between the tunnel and free air has only a negligible effect upon the profile drag. A better idea of the nature of the effect can be had by further examination of the difference between the two cases. It follows from equations (55) that, if the angles of attack in the tunnel and in free air are related as required by equation (54) or (64), the transposition of a given airfoil from free air to the tunnel is equivalent to increasing the coefficient A_1 for the airfoil in free air by an amount

$$\Delta A_1 = A_1' - A_1 = \frac{\sigma}{1 - M^2} (2A_0' + A_1')$$

which can be written to the first order as

$$\Delta A_1 = \frac{1}{\pi} \frac{\sigma}{1 - M^2} c_l$$

As can be seen from equation (46), this can be accomplished by maintaining the angle of attack unaltered in free air and changing the ordinate of the mean-camber line at every point by an amount Δy_c such that

$$\frac{d(\Delta y_c)}{dx} = \frac{1}{\pi} \frac{\sigma}{\sqrt{1 - M^2}} c_l \cos \theta \qquad (80)$$

The value of Δy as a fraction of the chord is then

$$\frac{\Delta y_c}{c} = \int \frac{d(\Delta y_c)}{dx} d\left(\frac{x}{c}\right) + C$$

which after substitution from equations (44) and (80) can be integrated to obtain

$$\frac{\Delta y_c}{c} = -\frac{1}{8\pi} \frac{\sigma}{\sqrt{1 - M^2}} c_l \cos 2\theta + C$$

The constant of integration C is determined by the condition that $\Delta y_c/c = 0$ at $\theta = 0$ and $\theta = \pi$. The equation for the change in the camber line then becomes finally

$$\frac{\Delta y_c}{c} = \frac{1}{\pi} \frac{\sigma}{\sqrt{1 - M^2}} c_l \left[\left(\frac{x}{c}\right) - \left(\frac{x}{c}\right)^2\right] \tag{81}$$

This is the equation of a parabola with vertex at the midchord point and has the same form as the equation for the camber line of an NACA conventional airfoil with maximum camber at the midchord point (reference 15). The maximum change in camber is

$$\left(\frac{\Delta y_c}{c}\right)_{max} = \frac{1}{4\pi} \frac{\sigma}{\sqrt{1 - M^2}} c_l \tag{82}$$

Thus, if the angles of attack of the airfoil in the tunnel and free air are adjusted as required by equations (64), the wall interference in the tunnel has the same effect upon the chordwise lift distribution as would an increase in camber in free air.

As a possible instance of a test for the determination of the drag of an airfoil of large chord at a low Mach number and low lift coefficient, consider the case of an airfoil in a tunnel providing a chord-height ratio of 0.5. The value of σ is then 0.051. Assume that the angle of attack α' in the tunnel is adjusted as required by equations (64) to correspond to an angle α giving a lift coefficient c_l of 0.3 in free air. Assuming that the Mach number is sufficiently low that the effect of

compressibility may be neglected in computing the tunnel-wall corrections, the change of maximum camber required in free air to duplicate the effect of the tunnel walls is given by equation (82) as

$$\left(\frac{\Delta y_c}{c}\right)_{max} = \frac{1}{4\pi}(0.051)(0.3) = 0.0012$$

An estimate based upon experimental data has been made of the effect upon the profile drag of a change in camber of this magnitude for an NACA conventional airfoil of moderate camber and 15-percent thickness with maximum camber at the midchord point. The result indicates that neglecting the effect upon the profile drag of the change in lift distribution caused by the tunnel walls leads in this case to an error in the final corrected drag coefficient of less than 0.0001. This is within the usual limits of experimental accuracy. The correction terms included in equation (67) amount in this instance to approximately 0.0004. If the chord-height ratio were increased to 1.0, the error in the drag coefficient would be increased to 0.0004, which is well outside the limits of experimental accuracy. This indicates the desirability of limiting the chord-height ratio if accurate measurements of the profile drag are desired, even at low values of the lift coefficient and Mach number. At higher values of the lift coefficient or Mach number the permissible chord-height ratio must be reduced correspondingly.

The foregoing comparison is based upon the specific case of an airfoil with maximum camber originally at the midchord point and is not necessarily applicable to other types of airfoils. For families of airfoils which have a smaller variation of drag with camber than do the NACA conventional sections, the error introduced by neglecting the effect of the change in lift distribution is correspondingly less. In any event, satisfactory accuracy can be obtained in the measurement of drag at low lift coefficients and Mach numbers by keeping the chord-height ratio within a suitable limit - say 0.7. A possible exception is an airfoil having an essentially flat pressure distribution in the region of transition from laminar to turbulent flow in the boundary layer. In such a case the changes in pressure gradient may shift the point of transition and noticeably alter the profile drag; however, for any such sensitive airfoil, alterations from this source are no more serious than similar changes which may accompany the small variations in pressure distribution caused in any practical application by irregularities in construction.

Some measure of the effect of the increment ΔP in chordwise lift distribution upon measurements of airfoil characteristics at high Mach numbers can be obtained by calculating the change in critical Mach number caused by this increment. Such a calculation has been made for an airfoil with minimum pressure originally at the midchord point. Since the increment ΔP is a maximum at midchord, this represents the worst possible case as regards the change in critical Mach number. For a chord-height ratio of 0.25, which is considerably larger than that ordinarily employed in tests at high Mach numbers, the critical Mach number was found to be reduced by approximately 0.001 at a lift coefficient of 0.3. A change of this magnitude is insignificant. It may be expected that the accompanying change in the aerodynamic coefficients in the vicinity of the critical Mach number will be correspondingly small.

THE PHENOMENON OF CHOKING

Consider the compressible adiabatic flow of a fluid in an elementary stream tube of varying area A_l, as shown in figure 5(a). Continuity of flow requires that the product $\rho_l V_l A_l$ be constant, where ρ_l, V_l, and A_l are the local values of density, velocity, and area, respectively, at any station along the tube. In consequence, the logarithmic derivative must vanish; that is,

$$\frac{d\rho_l}{\rho_l} + \frac{dV_l}{V_l} + \frac{dA_l}{A_l} = 0 \tag{83}$$

Bernoulli's equation for compressible flow requires that

$$\frac{dp_l}{\rho_l} = -V_l dV_l \tag{84}$$

where p_l is the local pressure. Defining V_{c_l} as the local velocity of sound, then

$$\frac{dp_l}{d\rho_l} = V_{c_l}^2$$

so equation (84) becomes, after substituting the value of dp_l in that equation,

$$\frac{d\rho_l}{\rho_l} = -\frac{V_l dV_l}{V_{c_l}^2} = -M_l^2 \frac{dV_l}{V_l}$$

where M_l is the local Mach number.

Substituting this relation into equation (83) gives

$$(1 - M_l^2)\frac{dV_l}{V_l} = -\frac{dA_l}{A_l} \tag{85}$$

From this well-known relation it is seen that at subsonic speeds the usual behavior associated with incompressible flow is obtained; namely, that as the area increases the velocity decreases. At supersonic speeds, however, the behavior is reversed in that as the area increases the velocity increases. When the local Mach number is unity it is seen that $dA = 0$; that is, if the velocity of sound is attained in the tube it can only be attained where the area has its minimum value.

When the local velocity of sound is attained at the minimum area section, the local Mach number at any other section, determined by the ratio of the area at that section to the minimum area, may be less or, in some cases, greater than unity depending upon the conditions promoting the flow in the tube. The nature of such flows can be studied by considering the change in the character of flow in the stream tube of figure 5(a) as the downstream pressure p_2 is decreased with respect to the upstream pressure p_1. If $p_1 - p_2$ is small so that completely subsonic flow is maintained in the tube, the nature of the velocity variation along the tube is that usually associated with incompressible flow as seen in curve I of figure 5(b). When $p_1 - p_2$ is increased so that sonic speed is just reached in the minimum area section, the variation of velocity along the tube becomes that shown in curve II. Any further decrease of the pressure p_2 cannot alter the flow upstream of the minimum area, since the velocity at the minimum section cannot exceed the velocity of sound. The only effect of decreasing the downstream pressure is to promote a supersonic flow region downstream of the minimum area, as shown by curve III of figure 5(b). This region is terminated by an abrupt return, through a compression shock wave, to subsonic flow.

The position of this terminal shock wave must be such as to bring about the necessary conversion of kinetic to thermal energy that is required to promote the downstream pressure p_2. For present purposes, the most important point concerning the flow as described is that when the velocity of sound is attained at the minimum area section, no further increase in the flow rate can be made regardless of the extent of the supersonic flow region downstream of this section. When this maximum flow rate has been reached, the stream tube is said to be "choked."

What has been said concerning the choking of a single stream tube applies to the complete system of stream tubes past an airfoil mounted in a two-dimensional-flow tunnel, as shown in figure 6. That is to say, when the velocity of the undisturbed flow far upstream in the tunnel reaches a certain value, sonic velocity is attained at the point of minimum area of each elementary stream tube between the airfoil and the upper wall of the tunnel. It is important to note that the locus of the points of minimum area of the separate stream tubes does not necessarily coincide with the shortest line between the airfoil and the upper wall. This is illustrated in figure 6, where the line A represents the shortest distance between the airfoil and the wall. If the conditions of flow were uniform across the stream at each chordwise station, the flow between the airfoil and the wall would be the same as in a single elementary stream tube, and sonic velocity would necessarily be attained along line A. In the actual case, however, the flow is two-dimensional, and sonic velocity is attained along some line, such as line B, not coincident with A. A similar situation exists in the space between the airfoil and the lower wall of the tunnel, where the sonic velocity is attained along some line D. As before, this line does not necessarily coincide with line C, the shortest line which can be drawn from the lower surface of the airfoil to the lower wall. (In order to avoid an apparent contradiction with the requirements of continuity, it must be kept in mind that the velocity vector is not, in general, perpendicular to either lines A and C or B and C.) Sonic speed is generally not attained coincidentally along lines B and D. Once it is attained along both these lines, however, the rate of flow past the airfoil in the tunnel can undergo no further increase. The Mach number of the flow ahead of the airfoil then has its maximum attainable value. This value is described as the "apparent choking Mach number."

In practice, the lines of sonic speed lie very close to the lines defining the shortest distance between the airfoil and the tunnel walls. For purposes of analysis, it will be assumed that

they are coincident, that is, that lines B and D coincide, respectively, with lines A and C. Under these conditions, the calculated rate of flow in the tunnel (which must in any event be equal to the rate of flow across lines A and C) will be somewhat greater than that which actually exists when the lines B and D have their true positions. The assumption of unidimensional flow will thus lead to a computed choking Mach number, which is slightly greater than the theoretically correct value.

On the basis of the foregoing assumption a relationship between the model size and the choking Mach number can be obtained from elementary considerations. The velocity V' and density ρ' of the flow far forward of the model, where the cross-sectional area is A', are constant across the stream. The velocity V_m and density ρ_m across the sonic-speed lines B and D of figure 6, where the area has the minimum value A_m, are again constant across the stream. The velocity V_m is the local sonic speed V_{c_m} so that the equation of continuity becomes

$$\rho'V'A' = \rho_m V_{c_m} A_m$$

Assuming adiabatic relations, the density and velocity terms can be related to the Mach number far upstream, which is now the apparent choking Mach number. The end result is that the ratio of the area of the undisturbed stream to the minimum flow area can be expressed in terms of the apparent choking Mach number M'_{ch} as

$$\frac{A'}{A_m} = \frac{1}{M'_{ch}} \left\{ 1 + \frac{\gamma-1}{\gamma+1} \left[(M'_{ch})^2 - 1 \right] \right\}^{\frac{\gamma+1}{2(\gamma-1)}} \tag{86}$$

The area ratio is clearly

$$\frac{A'}{A_m} = \frac{h}{h - t_p}$$

where h is the tunnel height and t_p the projected thickness of the airfoil normal to the flow direction. For reasons which will be evident later, the projected thickness in this relation will be replaced by an "effective" thickness t_e.

Taking the value for γ for air as 1.4, equation (86) becomes

$$\frac{t_e}{h} = 1 - \frac{M'_{ch}}{\left[1 + \frac{(M'_{ch})^2 - 1}{6}\right]^3} \qquad (87)$$

In figure 7, the ratio t_e/h is plotted as a function of the apparent choking Mach number. The region above the curve represents an impossible state of flow. As a matter of interest the results are shown for the supersonic- as well as the subsonic-flow regime, although for the purpose of this report only the subsonic choking Mach numbers will be considered.

In writing equation (87), the projected thickness was replaced by an effective thickness. If choking occurred as was assumed in the preceding analysis, then the effective thickness determining choking would be, of course, the projected thickness. In any real case, although the effective thickness may never be less than the projected thickness, it may be greater for two reasons. First, if the angle of attack is sufficiently large in absolute value, one of the lines B or D may move downstream of the trailing edge because of the continued contraction aft of the airfoil of the portion of the stream passing that line. Second, since on any aerodynamic body there exists, because of the action of viscosity, a boundary layer wherein the velocity must be reduced below the velocity in the otherwise unaffected flow field, it follows that the velocity of sound cannot be attained at those points close to the airfoil surface on the lines B and D of figure 6.

To estimate the choking Mach number in any practical case, it is necessary to assume that the effective thickness is equal to the projected thickness of the airfoil. Because of the possible contraction of part of the stream aft of the airfoil, as well as of the assumption that unidimensional flow exists as previously described, this procedure will lead to a computed choking Mach number which is greater than the theoretically correct value for an ideal, incompressible fluid. Further, the influence of the boundary layer will cause the actual choking Mach number to be even less than this theoretically correct value. Thus the use of the projected thickness in the computation may be expected to lead to an overestimation of the choking Mach number.

The effect of the boundary layer in this regard may best be illustrated by the case of a flat plate set at zero angle of attack in a two-dimensional-flow wind tunnel. Since the projected thickness is zero, the previously developed theory would indicate that no choking would occur in this case. Actually, because of the fact that the plate has a boundary layer and an accompanying wake, choking does occur, as is shown in the following discussion.

It was seen in the section on wake effect, wherein the effect of confining the wake of a body experiencing drag was considered, that when the influence of the wake spreads to the walls so that a uniform velocity field again exists, the temperature at this downstream position is related to the temperature upstream of the model by equation (13). Using equation (9), the ratio of the corresponding velocities may be seen to be

$$\frac{V''}{V'} = \frac{1 + \gamma(M')^2\left[1 - \frac{c_d'}{2}\left(\frac{c}{h}\right)\right]}{(\gamma + 1)(M')^2} - \frac{\sqrt{\left[1-(M')^2\right]^2 - \gamma(M')^2\,\frac{c_d'}{2}\left(\frac{c}{h}\right)\left\{2+\gamma(M')^2\left[2 - \frac{c_d'}{2}\left(\frac{c}{h}\right)\right]\right\}}}{(\gamma + 1)(M')^2} \tag{88}$$

The velocity ratio is imaginary when the sign of the group of terms under the radical is negative. The functional relationship between the choked Mach number and the drag-density factor $\tau c_d'$, found by equating the terms under the radical to zero and solving the resulting equation, is thus determined as

$$\tau c_d' = \frac{1 + \gamma(M'_{ch})^2}{2\gamma(M'_{ch})^2}\left\{1 - \sqrt{1 - \left[\frac{1 - (M'_{ch})^2}{1 + \gamma(M'_{ch})^2}\right]^2}\right\} \tag{89}$$

where, as before, $\tau = \frac{1}{4}\left(\frac{c}{h}\right)$. Setting $\gamma = 1.4$ for air gives

$$\tau c_d' = \frac{1+1.4(M'_{ch})^2}{2.8(M'_{ch})^2}\left\{1 - \sqrt{1 - \left[\frac{1 - (M'_{ch})^2}{1+1.4(M'_{ch})^2}\right]^2}\right\} \tag{90}$$

a graph of this function is shown on figure 8. The effect of drag on choking for supersonic as well as subsonic wind tunnels is shown as a matter of interest.

The manner in which drag promotes choking may be comprehended by examining the variations of the ratios V''/V' and T''/T' in equations (88) and (13) as the value of $\tau c_d'$ is increased. In the case of the subsonic wind tunnel, the effect of increasing $\tau c_d'$ is to increase V''/V'. On the other hand, T''/T' and hence V_c''/V_c' are reduced. Consequently, M''/M' is increased. In the case of the supersonic wind tunnel the effect of increasing $\tau c_d'$ is to decrease V''/V' and to increase T''/T' and hence V_c''/V_c'. Consequently, M''/M' is reduced in this case. In both cases choking occurs when the value of $\tau c_d'$ is such as to make the downstream Mach number M'' unity.

There is one definite limitation of the previous analysis in that it was assumed that the effective tunnel area remained constant at least until the wake had spread to the walls so that uniform flow conditions were obtained across the stream. Such a condition does not prevail in any conventional wind tunnel, nevertheless the results are useful in providing approximate values for the effect of drag as it determines choking. For example, a flat plate having an apparent drag coefficient of 0.007, if the chord-height ratio were 0.5, would choke a subsonic wind tunnel at a Mach number of 0.95 if choking occurred as assumed in the analysis. The serious influence of drag on choking for airfoils for which the drag coefficient may be many times this value is evident.

To summarize, it has been shown that choking will occur in a wind tunnel as a result of the confinement of the flow caused by the presence of the model and its wake. In the case of airfoils of normal thickness, choking will usually be determined by the effective dimensions of the body - that is, by the actual dimensions modified for the effects of boundary layer and stream contraction aft of the airfoil as previously described. Properly, the boundary-layer effect is a drag influence, but since its contribution is usually small it is most convenient to classify such confinement effects along with those due to the physical airfoil dimensions. In the case of very thin airfoils, at small angles of attack, choking will usually result from the confining effect of the wake rather than the effect of the airfoil thickness.

Once the choking Mach number is reached, no further increase in tunnel power can affect the apparent Mach number. Such an increase will only serve to extend the supersonic flow region downstream of the lines of sonic speed. The forces experienced by the airfoil at choking thus vary depending on the power input to the wind tunnel.

As a final consideration it should be noted that the flow in the tunnel at choking does not correspond to any real flow over an airfoil in free air. Since the choking Mach number approaches unity as the tunnel height h becomes infinite, flow in the tunnel at choking, if it is to correspond to any flow in free air, must correspond to the flow that would occur around an airfoil in a free stream moving at the velocity of sound. It can be demonstrated, however, that such a correspondence is impossible. Experimental evidence indicates that the flow conditions existing in the tunnel at choking are essentially steady state. That the flow about an airfoil in a free stream having the velocity of sound cannot be a steady-state flow can be readily shown. For instance, it was demonstrated previously that in any stream tube the velocity of sound, if it is attained at all, must be attained at the minimum area section. That is to say, the rate of flow per unit area is a maximum where the velocity is the velocity of sound. Now, presuppose a steady-state flow in the stream tubes in the vicinity of an airfoil in free air when the stream velocity is sonic speed. If the velocity either increases or decreases as the flow passes the airfoil, the stream tubes must expand. This is clearly impossible, since the disturbance to the flow would then increase continuously as the distance from the airfoil increases. On the other hand, if the velocity remains the velocity of sound in each stream tube, the streamlines will then have the same shape at all distances from the airfoil. Also, the pressure will remain constant throughout the entire flow field. This is, of course, impossible, since pressure differences are necessary to promote the required changes in the direction of flow past the airfoil. A steady-state flow similar to that observed in the tunnel at choking therefore cannot exist in free air at a free-stream Mach number of unity. Thus at the choking Mach number, the flow at the airfoil in the tunnel cannot correspond to any flow in free air. It follows that, at choking, the influence of the tunnel walls cannot be corrected for. Further, in the range of Mach numbers close to choking, where the flow is influenced to any extent by the incipient choking restriction, any correction for wall interference must be of doubtful validity.

That the flow at or close to choking cannot be corrected for the interference effects of the tunnel walls may be reasoned from another point of view. The assumption that it is permissible to correct wind-tunnel test data for the influence of the walls is justified only when the influence on the flow near the model is of such a uniform nature as not to alter the general character of the flow materially from some corresponding flow in free air. For instance, a velocity correction for wall interference may be

applied with confidence only if the velocity increment resulting from such interference is constant or nearly constant over that portion of the flow field wherein the influence of the model on the flow is important. Viewed in this light, it is clear that at or close to choking no correction can properly be applied, since an important influence of the model on the flow is felt over a range extending close or up to the walls, within which range the influence of the walls on the flow is not at all uniform.

It is thus clear that the equations which have been derived for correcting the test data obtained in a subsonic two-dimensional-flow wind tunnel for the effects of wall interference, cannot apply at the choking Mach number nor for a range of Mach numbers below the choking value. Moreover, when the model is not symmetrically disposed, the flow will, in general, attain sonic velocity across the stream on one side of the airfoil before it does on the other. In such cases, it is to be expected that the range of Mach numbers below choking for which the corrections are invalid is extended over that which would occur with a more nearly symmetrical flow pattern.

DISCUSSION

There is, at present, only a very limited amount of experimental data available which can be considered satisfactory for determining the accuracy of the theoretical interference corrections derived in this report. Moreover, none of the available data were obtained at sufficiently high Mach numbers to permit an evaluation of the accuracy of the theory with regard to the effect of compressibility.

In figure 9 are shown the experimentally determined variations of lift coefficient with angle of attack for several NACA 0012 airfoils, having different chord-height ratios. The data for those models for which the chord-height ratios are 0.25, 0.5, and 0.8 were obtained from tests in the 7- by 10-foot wind tunnel at the Ames Aeronautical Laboratory. These models were of 6-foot span mounted across the 7-foot dimension of the test section; 6-inch-span dummy ends were used in an attempt to obtain two-dimensional flow. A gap of about 1/32 inch occurred between the test panel, which was connected to the balance frame, and the dummy ends, which were fastened to the tunnel walls. The lift was determined both from force tests and by integration of chordwise pressure distributions at a section close to midspan. The data presented here are those obtained from the pressure distributions.

The data for the model for which the chord-height ratio is 1.0 were obtained from tests in the low-turbulence wind tunnel of the Langley Memorial Aeronautical Laboratory. This 3-foot-span model was fastened directly to the side walls of the tunnel such that no air gap existed, and the lift was determined from measurements of the reaction on the roof and floor of the test section. The test results for the various models are shown, uncorrected for tunnel-wall interference, in figure 5(a). In figure 5(b), are shown the same data corrected for wall interference by means of equations (62) and (64b). For all the models, the correction term depending upon $\tau c_d'$ is negligibly small. The test Reynolds numbers range from 2,000,000 to 6,000,000. It is seen that the corrected data obtained with the models for which (c/h) equals 0.25, 0.5, and 1.0 agree well with one another and with the section lift characteristics as obtained from tests in the NACA variable-density wind tunnel (reference 15). The data obtained with the model for which (c/h) equals 0.8, when corrected, indicate a lower lift-curve slope than do the other data. This is thought to be due to the effect of air leakage through the gaps at the ends of the test panel, the influence of which may be expected to become more pronounced as the chord of the airfoil is increased relative to the span.

In this regard, unreported tests in the Langley low-turbulence wind tunnel have shown that the presence of any gap through which leakage can occur will influence the aerodynamic characteristics to a surprisingly marked extent. This fact was also demonstrated by the Ames Laboratory tests on the NACA 0012 airfoils. A comparison of the lift characteristics obtained from balance measurements with those derived by integration of the pressure distributions, which are those given in figure 5, showed the lift-curve slopes for the former to be definitely lower than those for the latter. This indicates that the lift near the center of the test panel exceeded that at the sections near the gaps; that is, that the flow was definitely not two-dimensional.

In figure 6(a) is shown the experimental variation of lift coefficient with angle of attack for an NACA 23012 for which (c/h) equals 1.0. These data were obtained in the Langley low-turbulence wind tunnel at test Reynolds numbers of 4,560,000 and 6,450,000. The same data corrected for tunnel-wall interference by means of equations (62) and (64b) are shown in figure 6(b), together with section lift characteristics as obtained in the variable-density wind tunnel at an effective Reynolds number of 5,000,000 (reference 16). The corrected data are seen to be in excellent agreement with the results from the variable-density tunnel.

In figure 7(a) is shown the variation of quarter-chord-moment coefficient with lift coefficient for the NACA 0012 airfoils as obtained from the 7- by 10-foot wind-tunnel tests previously described. In figure 7(b) are shown the same data as corrected for the interference of the tunnel walls by means of equation (62) and (63). The section moment characteristics for this airfoil as obtained from tests in the variable-density wind tunnel (reference 15) are also shown for comparison. It is seen that the corrected data are in fair agreement with the data from the variable-density wind tunnel, except for the model for which (c/h) equals 0.8. It is believed that this disagreement is again due to the effects of air leakage through the gaps between the test panel and the dummy ends, and not to any shortcoming in the theory.

In figures 12 and 13, the uncorrected and corrected profile-drag coefficients for six symmetrical bodies at zero angle of attack are plotted as a function of the experimental chord-height ratio. The uncorrected experimental values c_d', shown by the crosses, are taken from results reported by Fage in reference 17. The theoretically corrected values c_d, indicated by the circled points, were computed from equation (67) for $M' = 0$. The extrapolated free-air value given in reference 17 for each of the bodies is indicated by a horizontal dashed line. It is seen that the corrected points are in good agreement with the extrapolated free-air values. In view of the assumptions made in the theoretical development, the relative accuracy of the corrections at large chord-height ratios and large drag coefficients is remarkable, particularly in the case of the circular cylinder.

Glauert (reference 2, pp. 56-57) suggests for the drag correction in an incompressible fluid a formula which may be written in the notation of this paper as

$$c_d = c_d' \left\{ 1 - 2\,\Lambda\sigma - 2\kappa \left(\frac{t}{c}\right)\left(\frac{c}{h}\right) \right\} \tag{91}$$

where (t/c) is the thickness ratio of the airfoil. In this equation, as in equation (67), the first correction term appears as a result of the interference between the airfoil thickness and the tunnel walls and is identical with the corresponding term in equation (67) for $M' = 0$. The remaining term is an empirical correction for the effect of the wake. The empirical factor κ is given by Glauert as a function of (c/t), the values being derived by fitting equation (91) to the experimental

data of reference 17. This wake term differs fundamentally from the wake correction of equation (67) in that the correction in this case consists of a single term which varies as (c/h); whereas the correction in equation (67) comprises two terms, one of which varies as (c/h) and one of which varies as $(c/h)^2$. Equation (67) gives corrected results which agree as closely with the free-air values as do the results obtained with equation (91). It has the advantage that it is generally applicable to all airfoils and does not depend upon the experimental results of tests of specific sections.

In summary, the corrected data of figures 5 to 9 indicate, for the most part, that when the flow is maintained strictly two-dimensional, the theoretical corrections for the tunnel-wall interference are, for low Mach numbers at least, accurate up to chord-height ratios of unity. The high accuracy observed at the larger values of (c/h) must, however, be regarded as fortuitous since the theoretical analysis is predicated upon the assumption that the chord-height ratio is small enough that all points of the airfoil may be assumed to lie on the center line of the tunnel and that powers of (c/h) higher than the second may be neglected. It is thought that, at low Mach numbers, chord-height ratios as high as 0.7 are permissible if the tests are conducted only for the purpose of obtaining drag characteristics at low values of the lift coefficient. However, care must be exercised in ascertaining the maximum chord-height ratio permissible in any particular case to insure that the interference lift represented by equation (63) is not of such nature and magnitude as to affect the general character of the flow in the boundary layer along the surface of the model. In tests conducted to determine the aerodynamic characteristics of a model up to and beyond the maximum lift, it is believed that the chord-height ratios must be kept to much lower values. At low Mach numbers, chord-height ratios up to 0.4 are probably permissible; however, there are no experimental data available at present to support this contention.

As noted previously, no experimental data could be found which would permit an evaluation of the accuracy of the calculated effects of compressibility upon the wall-interference corrections. Most certainly, as the test Mach numbers increase, the permissible chord-height ratios must decrease. Theory indicates that as long as the velocities induced at the position of the airfoil by the wall interference are small as compared with the velocity of the undisturbed stream, the corrections developed in this paper are valid even though the stream Mach number exceeds the critical for the airfoil under test. However, as previously

noted, at and for a range of Mach numbers below choking, the interference velocities are no longer small and the corrections are invalid. The extent of this range is unknown. It should be emphasized that the flow pattern at and in the immediate vicinity of choking does not correspond to any flow pattern obtainable with the airfoil in free air; so the test results in this range cannot be corrected by any method.

For zero Mach number (i.e., for an incompressible fluid), the results of the present paper can be compared with Goldstein's particular corrections for airfoils having small thickness and camber and small force coefficients. For an airfoil on the center line of the tunnel, equations (138), (139), (140), (143), and (144) of reference 3, together with the expressions of appendix 5 of reference 4, give the following equations for the velocity, angle of attack, and aerodynamic coefficients in an incompressible fluid:

$$\left.\begin{aligned} V &= V'\left\{1 + \sigma\,(2C_0 - C_2)\right\} \\ \alpha &= \alpha' + \frac{\sigma}{2\pi}\left\{c_l' + 4\left(c_{m_{\frac{c}{2}}}\right)_0\right\} \\ c_l &= c_l'\left\{1 - \sigma\right\} \\ c_d &= c_d'\left\{1 - 3\sigma\left(2C_0 - C_2\right)\right\} \\ c_{m_{\frac{c}{2}}} &= c_{m_{\frac{c}{2}}}' \end{aligned}\right\} \qquad (92)$$

Here, the moment coefficients are for moments about the midchord, and $\left(c_{m_{\frac{c}{2}}}\right)_0$ is the moment coefficient at zero lift in free air.

The quantities C_0 and C_2' are determined by the shape of the base profile according to the equations

$$\left.\begin{aligned} c_0 &= \frac{2}{\pi}\int_0^{\pi} \frac{y_t}{c}\,\frac{d\theta}{\sin\theta} \\ c_2 &= \frac{4}{\pi}\int_0^{\pi} \frac{y_t}{c}\,\frac{\cos 2\theta}{\sin\theta}\,d\theta \end{aligned}\right\} \tag{93}$$

In deriving these equations, the notation of references 3 and 4 has been changed to agree with that of the present paper, and the lift-curve slope in free air assumed to have its theoretical value of 2π.

The corresponding corrections as obtained by setting $M' = 0$ in equations (26), (62), (63), (64a), and (67) of the present paper are

$$\left.\begin{aligned} V &= V'\left\{1 + \Lambda\sigma + \tau c_d'\right\} \\ \alpha &= \alpha' + \frac{\sigma}{2\pi}\left\{c_l' + 4c_{m_{\frac{c}{4}}}'\right\} \\ c_l &= c_l'\left\{1 - \sigma - 2\Lambda\sigma - 2\tau c_d'\right\} \\ c_d &= c_d'\left\{1 - 3\Lambda\sigma - 2\tau c_d'\right\} \\ c_{m_{\frac{c}{2}}} &= c_{m_{\frac{c}{2}}}'\left\{1 - 2\Lambda\sigma - 2\tau c_d'\right\} \end{aligned}\right\} \tag{94}$$

The last of these equations is obtained from equations (62) and (63) by means of the relation $c_{m_{\frac{c}{2}}} = c_{m_{\frac{c}{4}}} + \frac{1}{4}\,c_l$.

The correction terms involving σ in the two equations for the velocity are equivalent, except that the factor Λ, which

appears in the equation of the present paper, is replaced in Goldstein's equation by the quantity $(2C_0 - C_2)$. Equation (93) gives

$$(2C_0 - C_2) = \frac{4}{\pi}\int_0^{\pi} \frac{y_t}{c} \frac{1 - \cos 2\theta}{\sin\theta} d\theta = \frac{8}{\pi}\int_0^{\pi} \frac{y_t}{c} \sin\theta \, d\theta$$

which becomes, after substitution from equation (44),

$$(2C_0 - C_2) = \frac{16}{\pi}\int_0^1 \left(\frac{y_t}{c}\right) d\left(\frac{x}{c}\right) = \frac{8}{\pi}\frac{A}{c^2} \qquad (95)$$

where A is the cross-sectional area of the airfoil. The factor Λ can be expressed in analogous form by means of equation (19.05) of reference 2. Since $\frac{1}{4}\Lambda c^2$ is equivalent to the quantity λt^2 in reference 2, this equation becomes

$$\Lambda = \frac{8}{\pi}\frac{A + A_v}{c^2} \qquad (96)$$

where A_v is the so-called "virtual area" of the base profile. The virtual area of a given body in two-dimensional flow is defined as the area occupied by a fictitious quantity of fluid having a uniform density ρ and velocity V and possessing a kinetic energy equal to the total kinetic energy of the field of flow about the same body when it is moving forward with a steady velocity V through an unlimited expanse of incompressible fluid of density ρ. The magnitude of the virtual area depends upon the shape as well as upon the size of the body. It is seen that the first correction term in the velocity equation of the present paper (which for the incompressible case is simply the result originally derived by Lock) has a somewhat higher value than the correction term of the Goldstein equation. The Goldstein equation contains no term corresponding to the term $\tau c_d'$ in the equation of the present paper. Goldstein includes this correction, however, in the equation for the determination of the stream velocity from measurements made at the tunnel wall upstream of the model.

The Goldstein equation for the correction of the measured drag coefficient likewise differs from that of the present paper

by the replacement of the factor Λ by the quantity $(2C_0 - C_2)$ and by the omission of the term in $\tau c_d'$. If Goldstein's equation is applied to the experimental results of Fage given in figures 12 and 13, it is found that there is little to choose between the corrected results given by the two equations, except in the case of the circular cylinder where the results obtained from the equation of the present paper are better.

The corrections to the lift and moment coefficients as derived by Goldstein differ markedly from those of the present paper in that Goldstein's equations contain no terms corresponding to the $2\Lambda\sigma$ and $2\tau c_d'$ terms which appear in the equations of this paper. As has been noted previously, the $2\tau c_d'$ term is accounted for indirectly in the determination of the apparent stream velocity. A term of the type $2\Lambda\sigma$ is necessary, however, to correct the measured coefficients for the increase in dynamic pressure caused by the interference between the walls and the airfoil thickness.

Since the moment coefficient at zero lift is the same about any axis and since the change from the free air to the measured moment coefficient in the correction to the angle of attack will introduce only differences of the second order in σ, Goldstein's equation for the corrected angle of attack may be written with sufficient accuracy as

$$\alpha = \alpha' + \frac{\sigma}{2\pi}\left[c_l' + 4\left(c_{m_{\frac{c}{4}}}'\right)_0\right]$$

In this equation, the part of the correction due to the moment on the airfoil is constant, its value depending only upon $c_{m_{\frac{c}{4}}}'$ for zero lift; whereas in the corresponding equation of the present paper the part of the correction due to the moment varies with the angle of attack. This difference is of small consequence in most applications; however, the equation of the present paper, which includes the actual variation in moment, may be somewhat the more accurate, especially at high angles of attack.

The compressibility factors which appear in the complete equations of the present paper are comparable with the results of Goldstein and Young (reference 5). The equation for drag as given

in reference 5, when expressed in coefficient form and altered to agree with the notation of the present paper, can be written

$$c_d = c_{d'} \left\{ 1 - \frac{2}{\left[1-(M')^2\right]^{3/2}} \Lambda\sigma - \frac{1}{\left[1-(M')^2\right]^{3/2}} 2\kappa \left(\frac{t}{h}\right) \right\} \qquad (97)$$

This equation is obtained by modifying equation (91) to include the effect of compressibility. Comparison of the compressibility modifications of equation (97) with those of the corresponding terms of equation (67) reveals that the compressibility factors appearing in the first correction terms differ by the inclusion of a term $-(M')^2$ in the numerator in equation (67). This difference arises from a failure to note in the development of equation (97) that in a compressible fluid the dynamic pressure in the tunnel is affected by the change in density which accompanies the change in axial velocity. The compressibility factor of the second (or wake-correction) term of equation (97) is not comparable with the compressibility factors of the wake-correction terms of equation (67) because of the fundamental difference in the nature of the corrections already pointed out in the discussion of equation (91). The compressibility factors in the equations for lift, moment, and angle of attack in reference 5 agree with those appearing in the corresponding terms of the equations of the present paper. It should be noted, however, that the lift and moment equations of reference 5 include no corrections for the difference between the true and apparent dynamic pressures in the tunnel.

CONCLUSIONS

Airfoil data obtained from tests in a two-dimensional-flow wind tunnel can be corrected to free-air conditions by means of the following equations:

$$V = V' \left\{ 1 + \frac{1}{\left[1-(M')^2\right]^{3/2}} \Lambda\sigma + \frac{1 + 0.4\,(M')^2}{1 - (M')^2} \tau c_{d'} \right\} \qquad (26)$$

$$q = q' \left\{ 1 + \frac{2 - (M')^2}{\left[1-(M')^2\right]^{3/2}} \Lambda\sigma + \frac{\left[2-(M')^2\right]\left[1+0.4(M')^2\right]}{1 - (M')^2} \tau c_{d'} \right\} \qquad (29)$$

$$R=R'\left\{1+\frac{1-0.7(M')^2}{\left[1-(M')^2\right]^{3/2}}\Lambda\sigma+\frac{\left[1-0.7(M')^2\right]\left[1+0.4(M')^2\right]}{1-(M')^2}\tau c_d'\right\} \quad (32)$$

$$M=M'\left\{1+\frac{1+0.2(M')^2}{\left[1-(M')^2\right]^{3/2}}\Lambda\sigma+\frac{\left[1+0.2(M')^2\right]\left[1+0.4(M')^2\right]}{1-(M')^2}\tau c_d'\right\} \quad (33)$$

$$\alpha=\alpha'+\frac{57.3\sigma}{2\pi\sqrt{1-(M')^2}}\left\{c_l'+4c_{m_{\frac{c}{4}}}'\right\} \quad \text{(degrees)} \quad (64b)$$

$$c_l=c_l'\left\{1-\frac{\sigma}{1-(M')^2}-\frac{2-(M')^2}{\left[1-(M')^2\right]^{3/2}}\Lambda\sigma-\frac{\left[2-(M')^2\right]\left[1+0.4(M')^2\right]}{1-(M')^2}\tau c_d'\right\} \quad (62)$$

$$c_{m_{\frac{c}{4}}}=c_{m_{\frac{c}{4}}}'\left\{1-\frac{2-(M')^2}{\left[1-(M')^2\right]^{3/2}}\Lambda\sigma-\frac{\left[2-(M')^2\right]\left[1+0.4(M')^2\right]}{1-(M')^2}\tau c_d'\right\}+c_l'\frac{\sigma}{4\left[1-(M')^2\right]} \quad (63)$$

$$c_d=c_d'\left\{1-\frac{3-0.6(M')^2}{\left[1-(M')^2\right]^{3/2}}\Lambda\sigma-\frac{\left[2-(M')^2\right]\left[1+0.4(M')^2\right]}{1-(M')^2}\tau c_d'\right\} \quad (67)$$

where

$$\tau=\frac{1}{4}\left(\frac{c}{h}\right)$$

$$\sigma=\frac{\pi^2}{48}\left(\frac{c}{h}\right)^2$$

and Λ is a dimensionless factor the value of which depends upon the shape of the base profile of the airfoil. (See equation (3) and table I.) The remaining symbols are defined in appendix B. Numerical values of the functions of M' which appear in these

equations are given in table II. Experimental pressure distributions also can be corrected by a method outlined in the text.

The corrections derived should be valid theoretically up to a Mach number near the choking value, which is the maximum Mach number attainable in the wind tunnel. The choking Mach number is shown to be the stream Mach number at which a Mach number of unity is attained locally across the tunnel either (1) at the position of the airfoil because of the reduction of the available flow area occasioned by the presence of the airfoil, or (2) downstream of the airfoil as a result of the influence of the airfoil drag upon the flow in the wake. The choking Mach number can be estimated by means of equations presented in the report.

Insofar as can be ascertained from the small amount of experimental data available, the correction equations are applicable at low Mach numbers for values of the chord-height ratio (c/h) as high as 0.7 if the tests are conducted for the purpose of obtaining drag characteristics at low values of the lift coefficient. In tests conducted to determine the aerodynamic characteristics of an airfoil up to and beyond the maximum lift, it is thought that a chord-height ratio of 0.4 is permissible at low Mach numbers, although there is no experimental evidence to support this contention at present. At high Mach numbers the permissible chord-height ratios must logically be expected to decrease. In particular, if the critical speed is exceeded, it is probable that only very small values of (c/h) are permissible. There are at this time no experimental data available on this aspect of the problem.

Comparison of the results of the present paper with those of references 3, 4, and 5 reveals certain differences as noted in the section Discussion.

Ames Aeronautical Laboratory,
National Advisory Committee for Aeronautics,
Moffett Field, Calif.

APPENDIX A

THE VELOCITY FIELD FOR A SOURCE AND FOR A SYMMETRICAL AIRFOIL IN A COMPRESSIBLE STREAM

The velocity induced at a point in a compressible fluid stream by a single fluid source can be found to a first degree of approximation by a modification of the method used by Glauert (reference 7) for the consideration of a vortex in a compressible fluid. To this end, a system of polar coordinates is introduced. The origin is located at the source and the polar axis extends downstream parallel to the velocity V of the undisturbed stream. (See fig. 14.) The resultant velocity U at any point $L(r,\varphi)$ is defined by the velocity components w and n parallel and normal, respectively, to the radius vector.

The condition for irrotational motion requires that at all points in the field

$$\frac{\partial(rn)}{\partial r} - \frac{\partial w}{\partial \varphi} = 0 \tag{A1}$$

The equation of continuity is

$$\frac{\partial(rw)}{\partial r} + \frac{\partial n}{\partial \varphi} + \frac{rw}{\rho_l}\frac{\partial \rho_l}{\partial r} + \frac{n}{\rho_l}\frac{\partial \rho_l}{\partial \varphi} = 0 \tag{A2}$$

where ρ_l is the density of the fluid at any point.

The source strength (mass flow per unit time) is denoted by Q. Then, for any circle enclosing the source, considerations of symmetry and continuity, respectively, provide the two integral relationships

$$\int_0^{2\pi} nr \, d\varphi = 0 \tag{A3}$$

and

$$\int_0^{2\pi} \rho_l wr \, d\varphi = Q \tag{A4}$$

The radial and circumferential components of the velocity may be expanded in the series

$$w = V\left(\cos\varphi + \sum_{s=1}^{\infty}\frac{A_s}{r^s}\right)$$

$$n = -V\left(\sin\varphi + \sum_{s=1}^{\infty}\frac{B_s}{r^s}\right)$$

where A_s and B_s are functions of φ. If r is large, it is sufficient to retain only the first terms of each power series, so that

$$\left.\begin{aligned} w &= V\left(\cos\varphi + \frac{A}{r}\right) \\ n &= -V\left(\sin\varphi + \frac{B}{r}\right) \end{aligned}\right\} \qquad (A5)$$

To the first power in $(1/r)$, the square of the resultant velocity is

$$\left(\frac{U}{V}\right)^2 = \frac{w^2 + n^2}{V^2} = 1 + \frac{2}{r}(A\cos\varphi + B\sin\varphi)$$

For reversible adiabatic flow, the local density ρ_l is related to the density ρ of the undisturbed stream by

$$\rho_l = \rho\left\{1 - \frac{\gamma - 1}{2}M^2\left[\left(\frac{U}{V}\right)^2 - 1\right]\right\}^{\frac{1}{\gamma - 1}}$$

where M is the Mach number of the undisturbed stream and γ is the ratio of the specific heats. Thus, to the first power in $(1/r)$,

$$\rho_l = \rho\left\{1 - \frac{M^2}{r}(A\cos\varphi + B\sin\varphi)\right\} \qquad (A6)$$

The solution is now obtained by inserting values from expressions (A5) and (A6) into the fundamental equations. Substitution of (A5) into the equation for irrotational motion (A1) requires that A shall be a constant. Substitution of (A5) and (A6) into the equation of continuity then gives

$$\frac{dB}{d\varphi}(1 - M^2 \sin^2 \varphi) = M^2 (A \cos 2\varphi + B \sin 2\varphi)$$

which becomes upon integration

$$B(1 - M^2 \sin^2 \varphi) = \frac{1}{2} M^2 A \sin 2\varphi + C \tag{A7}$$

where C is a constant. The integral equations (A3) and (A4) become, respectively,

$$\int_0^{2\pi} B d\varphi = 0 \tag{A8}$$

and

$$\frac{M^2}{2} \int_0^{2\pi} B \sin 2\varphi \, d\varphi = 2\pi A \left(1 - \frac{M^2}{2}\right) - \frac{Q}{\rho V} \tag{A9}$$

Substitution of the expression for B from equation (A7) into the integral equation (A9) gives

$$A = \frac{Q}{2\pi\rho V}\left[\frac{1}{\sqrt{1 - M^2}}\right]$$

while substitution into equation (A8) shows that C = 0. Thus, from equation (A7),

$$B = \frac{Q}{4\pi\rho V}\left[\frac{M^2 \sin 2\varphi}{(1 - M^2 \sin^2\varphi)\sqrt{1 - M}}\right]$$

The expressions for the velocity components therefore become

$$\left.\begin{aligned} w &= V\cos\varphi + \frac{Q}{2\pi\rho r}\left[\frac{1}{\sqrt{1-M^2}}\right] \\ n &= -V\sin\varphi - \frac{Q}{2\pi\rho r}\left[\frac{M^2\sin\varphi\cos\varphi}{(1-M^2\sin^2\varphi)\sqrt{1-M^2}}\right] \end{aligned}\right\} \quad (A10)$$

For a Mach number of zero these equations reduce to the well-known results for a source in an incompressible fluid.

From equations (A10) the velocity components u and v, parallel and perpendicular, respectively, to the direction of the undisturbed stream, are found to be

$$\left.\begin{aligned} u &= V + \frac{Q}{2\pi\rho r}\left[\frac{\cos\varphi}{\sqrt{1-M^2}\,(1-M^2\sin^2\varphi)}\right] \\ v &= \frac{Q}{2\pi\rho r}\left[\frac{\sqrt{1-M^2}\sin\varphi}{1-M^2\sin^2\varphi}\right] \end{aligned}\right\} \quad (A11)$$

The drag experienced by the source can be determined by evaluating the integral

$$D = -\int_0^{2\pi}\left\{p_l\cos\varphi + \rho_l w(w\cos\varphi - n\sin\varphi)\right\} r\,d\varphi$$

over any circle enclosing the source. To the accuracy previously employed, the pressure at any point is

$$p_l = p - \frac{\rho V^2}{r}(A\cos\varphi + B\sin\varphi) \quad (A12)$$

Insertion of this expression, together with (A5) and (A6), into the equation for drag gives finally

$$D = -VQ \quad (A13)$$

which is the same as for a source in an incompressible fluid. It is apparent from considerations of symmetry that the lift force of the source is zero.

The results of equations (A11) can be used to study the field of flow about a symmetrical airfoil at zero angle of attack in a uniform stream. Such an airfoil can be represented by a suitable system of sources and sinks distributed continuously along the chord line. If the notation of figure 15 is used, the vertical velocity v_i induced in an incompressible stream at a given point (x_o, y_o) on the surface of the airfoil is

$$v_i = \frac{1}{2\pi\rho}\int_0^c \frac{\sin\varphi}{r}\left(\frac{dQ_i}{dx}\right) dx = \frac{1}{2\pi\rho}\int_0^c \frac{y_o}{(x_o-x)^2+y_o^2}\left(\frac{dQ_i}{dx}\right) dx \quad (A14)$$

where $\left(\frac{dQ_i}{dx}\right)$ is the strength per unit length of the source-sink distribution in an incompressible stream. From the second of equations (A11) it follows that the velocity v_c at the same point in a compressible stream is

$$v_c = \frac{1}{2\pi\rho}\int_0^c \frac{\sqrt{1-M^2}\sin\varphi}{r(1-M^2\sin^2\varphi)}\left(\frac{dQ_c}{dx}\right) dx$$

or

$$v_c = \frac{\sqrt{1-M^2}}{2\pi\rho}\int_0^c \frac{y_o}{(x_o-x)^2 + (1-M^2)y_o^2}\left(\frac{dQ_c}{dx}\right) dx \quad (A15)$$

where $\left(\frac{dQ_c}{dx}\right)$ is the strength of the source-sink distribution in the compressible case. For any given airfoil of small thickness the condition that the flow shall be tangential to the surface of the airfoil requires that $v_c = v_i$ at all points on the surface. This fact can be used to relate the source-sink distributions for a thin airfoil in the compressible and incompressible streams by considering the limiting forms of equations (A14) and (A15) as y_o approaches zero.

Consider first the limiting form of equation (A14), which may be written

$$v_i = \lim_{y_o \to 0} \frac{y_o}{2\pi\rho}\int_0^c \frac{1}{(x_o-x)^2 + y_o^2}\left(\frac{dQ_i}{dx}\right) dx \quad (A16)$$

It is seen that even for $y_o = 0$ the integral in this equation is finite when evaluated over any interval of integration not including the point $x = x_o$. In the limit, the contribution of such intervals to the right-hand side of the equation is therefore zero, and the equation may be written

$$v_i = \lim_{\epsilon \to 0} \lim_{y_o \to 0} \frac{y_o}{2\pi\rho} \int_{x_o-\epsilon}^{x_o+\epsilon} \frac{1}{(x_o - x)^2 + y_o^2} \left(\frac{dQ_i}{dx}\right) dx$$

In evaluating the limit in this equation, care must be taken that the limit with respect to y_o is taken first in every case. Integration by parts gives

$$v_i = \lim_{\epsilon \to 0} \lim_{y_o \to 0} \frac{1}{2\pi\rho} \left\{ - \left(\frac{dQ_i}{dx}\right) (\tan^{-1}) \frac{x_o - x}{y_o} \Bigg|_{x_o-\epsilon}^{x_o+\epsilon} + \int_{x_o-\epsilon}^{x_o+\epsilon} \left(\frac{d^2Q_i}{dx^2}\right) (\tan^{-1}) \frac{x_o-x}{y_o} dx \right\} \quad (A17)$$

By virtue of the first mean value theorem for integrals (reference 18, p. 65) the integral term in this equation may be written

$$\int_{x_o-\epsilon}^{x_o+\epsilon} \left(\frac{d^2Q_i}{dx^2}\right)(\tan^{-1})\frac{x_o-x}{y_o}dx = \left(\frac{d^2Q_i}{dx^2}\right)_{x=\xi_1} \int_{x_o-\epsilon}^{x_o} (\tan^{-1})\frac{x_o-x}{y_o} dx + \left(\frac{d^2Q_i}{dx^2}\right)_{x=\xi_2} \int_{x_o}^{x_o+\epsilon} (\tan^{-1})\frac{x_o-x}{y_o} dx$$

where $(x_o-\epsilon) \leqq \xi_1 \leqq x_o$ and $x_o \leqq \xi_2 \leqq (x_o+\epsilon)$. The division into two integrals is necessary to ensure that the conditions under which the mean-value theorem is applicable are fulfilled; namely,

that $\left(\frac{d^2Q_i}{dx^2}\right)$ is continuous and that $(\tan^{-1})\frac{x_o - x}{y_o}$ has the same sign throughout the interval of integration. Integration gives

$$\int_{x_o-\epsilon}^{x_o+\epsilon} \left(\frac{d^2Q_i}{dx^2}\right)(\tan^{-1})\frac{x_o-x}{y_o}\,dx = \left[\left(\frac{d^2Q_i}{dx^2}\right)_{x=\xi_1} - \left(\frac{d^2Q_i}{dx^2}\right)_{x=\xi_2}\right] \times \left[\epsilon\,(\tan^{-1})\frac{\epsilon}{y_o} - \frac{y_o}{2}\log\left(1+\frac{\epsilon^2}{y_o^2}\right)\right]$$

In the limit, the value of the terms in the second bracket in zero. Thus, only the first term need be retained in equation (A17), which may now be written

$$v_i = \lim_{\epsilon \to 0}\ \lim_{y_o \to 0}\ \frac{1}{2\pi\rho}(\tan^{-1})\frac{\epsilon}{y_o}\left[\left(\frac{dQ_i}{dx}\right)_{x=x_o+\epsilon} + \left(\frac{dQ_i}{dx}\right)_{x=x_o-\epsilon}\right]$$

$$= \frac{1}{\pi\rho}\left(\frac{dQ_i}{dx}\right)_{x=x_o} \lim_{\epsilon \to 0}\ \lim_{y_o \to 0}\ (\tan^{-1})\frac{\epsilon}{y_o}$$

Thus the limiting form of equation (A14) becomes finally

$$v_i = \frac{1}{2\rho}\left(\frac{dQ_i}{dx}\right) \qquad \text{(A18)}$$

where v_i and $\left(\frac{dQ_i}{dx}\right)$ may now be considered as pertaining to the same general chordwise station x.

The limiting form of equation (A15) can be found in similar fashion. In this case integration by parts gives in place of equation (A17)

$$v_c = \lim_{\epsilon \to 0} \lim_{y_o \to 0} \frac{\sqrt{1 - M^2}}{2\pi\rho} \left\{ -\left(\frac{dQ_c}{dx}\right) \frac{1}{\sqrt{1 - M^2}} (\tan^{-1}) \frac{x_o - x}{y_o \sqrt{1-M^2}} \Bigg|_{x_o - \epsilon}^{x_o + \epsilon} \right.$$

$$\left. + \int_{x_o - \epsilon}^{x_o + \epsilon} \left(\frac{d^2 Q_c}{dx^2}\right) \frac{1}{\sqrt{1 - M^2}} (\tan^{-1}) \frac{x_o - x}{y_o \sqrt{1 - M^2}} \, dx \right\} \quad (A19)$$

As before, the value of the integral term in this equation is zero. The limiting form of equation (A15) becomes finally

$$v_c = \frac{1}{2\rho} \left(\frac{dQ_c}{dx}\right) \quad (A20)$$

which is the same as (A18).

Since for any given airfoil $v_c = v_i$ at all chordwise stations, it follows from (A18) and (A20) that

$$\left(\frac{dQ_c}{dx}\right) = \left(\frac{dQ_i}{dx}\right) \quad (A21)$$

that is, the source-sink distributions necessary to represent any given thin symmetrical airfoil in a uniform stream are identical for the compressible and incompressible case.

This result can be used to calculate the effect of compressibility upon the field of induced velocities at a considerable distance from the airfoil. The increase in longitudinal velocity at a large distance y_1 directly above or below the midchord point of the airfoil in an incompressible fluid is approximately

$$(u_i - V) = \frac{1}{2\pi\rho y_1^2} \int_0^c \left(\frac{c}{2} - x\right) \left(\frac{dQ_i}{dx}\right) dx$$

By virtue of the first of equations (A11), the corresponding velocity at the same point in a compressible fluid is approximately

$$(u_c - V) = \frac{1}{2\pi\rho y_1^2 (1 - M^2)^{3/2}} \int_0^c \left(\frac{c}{2} - x\right)\left(\frac{dQ_c}{dx}\right) dx$$

Thus, in view of equation (A21),

$$(u_c - V) = \frac{1}{(1 - M^2)^{3/2}} (u_i - V) \tag{A22}$$

that is, in a compressible fluid the increase in longitudinal velocity at a point a considerable distance directly above or below a symmetrical airfoil is $1/(1 - M^2)^{3/2}$ times the increase in longitudinal velocity at the same point in an incompressible fluid.

The foregoing results can be used also to determine the effect of compressibility upon the drag of an airfoil in a stream having a longitudinal pressure gradient. Consider an undisturbed nonuniform stream having at some given point a velocity V, a density ρ, and a streamwise pressure gradient dp/dx. By virtue of Bernoulli's equation, there must be at this point a velocity gradient

$$\frac{dV}{dx} = \frac{1}{\rho V}\frac{dp}{dx} \tag{A23}$$

This holds true both in the compressible and the incompressible case. The velocity v a small distance x from the point in question is then

$$v = V + x\frac{dV}{dx} = V - \frac{x}{\rho V}\frac{dp}{dx} \tag{A24}$$

As a result of equation (A13), the drag experienced by an airfoil placed at this point in the stream is, for both the compressible and incompressible cases,

$$D = -\int_0^c v\left(\frac{dQ}{dx}\right)dx = -V\int_0^c \left(\frac{dQ}{dx}\right)dx + \frac{1}{\rho V}\frac{dp}{dx}\int_0^c x\left(\frac{dQ}{dx}\right)dx$$

where (dQ/dx) is, as before, the strength per unit length of the source-sink system necessary to represent the airfoil. In order to fulfill the condition that the airfoil is a closed body, the source-sink system must be such that

$$\int_0^c \left(\frac{dQ}{dx}\right) dx = 0$$

Thus the drag is finally

$$D = \frac{1}{\rho V} \frac{dp}{dx} \int_0^c x \left(\frac{dQ}{dx}\right) dx \qquad \text{(A25)}$$

in both the compressible and the incompressible cases. If the streamwise pressure gradient is small, equation (A21) is still applicable; that is, the source-sink distributions necessary to represent the airfoil in the compressible and incompressible cases are identical. It therefore follows from equation (A25) that the drag of an airfoil in a stream having a longitudinal pressure gradient is unaffected by fluid compressibility.

APPENDIX B

LIST OF IMPORTANT SYMBOLS

c airfoil chord

t airfoil thickness

h tunnel height

Λ a factor depending upon shape of base profile (see equation (3) and table I)

σ $\frac{\pi^2}{48}\left(\frac{c}{h}\right)^2$; factor depending upon size of airfoil relative to tunnel

τ $\frac{1}{4}\left(\frac{c}{h}\right)$; factor depending upon size of airfoil relative to tunnel

α angle of attack

c_l section lift coefficient

$c_{m_{\frac{c}{4}}}$ section quarter-chord-moment coefficient

$c_{m_{\frac{c}{2}}}$ section midchord-moment coefficient

c_d section drag coefficient

V stream velocity

M Mach number

M'_{ch} apparent Mach number at choking

R Reynolds number

γ $\frac{c_p}{c_v}$; ratio of specific heat of gas at constant pressure to to specific heat at constant volume (for air $\gamma = 1.4$)

H total head

p static pressure

q dynamic pressure

ρ mass density

μ coefficient of viscosity

T absolute temperature

V_c speed of sound

$1+\eta$ compressibility factor (see equation (71) and fig. 4)

D section drag

ΔD section drag due to streamwise pressure gradient

P chordwise lift distribution in coefficient form

P_e interference lift distribution (see equation (78) and table III)

P_l local pressure coefficient (see equation (69))

S_l local pressure coefficient (see equation (68))

x coordinate of points on chord line as measured from leading edge

θ angular coordinate of points on chord line (see equation (43))

r radial distance in polar coordinates

φ polar angle in polar coordinates (positive counterclockwise)

t_p projected thickness of airfoil

t_e effective thickness of airfoil

y_t ordinate of base profile

$\frac{dy_c}{dx}$ slope of mean-camber line

Q source strength

$\frac{d\Gamma}{dx}$ vorticity per unit length of chord line

u horizontal component of velocity

v vertical component of velocity

n circumferential component of velocity in polar coordinates (positive counterclockwise)

w radial component of velocity in polar coordinates

A geometrical area of airfoil section

A_v virtual area of airfoil section

A' cross-sectional area of empty tunnel

A_m minimum cross-sectional area between model and tunnel walls

A_l local cross-sectional area of stream tube

A_n Fourier coefficients (see equations (45) and (49))

Superscripts.

(') when pertaining to fluid properties, denotes values existing in tunnel far upstream from model; when pertaining to airfoil characteristics, denotes values in tunnel, coefficients being referred to apparent dynamic pressure q'

(") denotes fluid properties far downstream from model

(*) denotes airfoil characteristics in tunnel as coefficients referred to true dynamic pressure q

Subscripts

c denotes values in compressible fluid (excepting V_c)

i denotes values in incompressible fluid

l denotes local conditions at point in fluid

s denotes conditions existing far downstream when airfoil and wake are replaced by source

m denotes conditions at minimum cross-sectional area between airfoil and tunnel walls

L denotes values on lower surface of airfoil

U denotes values on upper surface of airfoil.

REFERENCES

1. Lock, C. N. H.: The Interference of a Wind Tunnel on a Symmetrical Body. R. & M. No. 1275, British A.R.C., 1929.

2. Glauert, H.: Wind Tunnel Interference on Wings, Bodies and Airscrews. R. & M. No. 1566, British A.R.C., 1933.

3. Goldstein, S.: Two-Dimensional Wind-Tunnel Interference. 6157 Ae. 2075, British A.R.C. (British Confidential-U. S. Restricted), Sept. 29, 1942.

4. Goldstein, S.: Steady Two-Dimensional Flow past a Solid Cylinder in a Non-Uniform Stream. 6167 Ae. 2084 F.M. 554, British A.R.C. (British Confidential - U. S. Restricted). Oct. 5, 1942.

5. Goldstein, S., and Young, A. D.: The Linear Perturbation Theory of Compressible Flow, with Applications to Wind-Tunnel Interference. 6865 Ae, 2262 F.M. 601, British A.R.C. (British Confidential - U. S. Restricted), July 6, 1943.

6. Allen, H. Julian: A Simplified Method for the Calculation of Airfoil Pressure Distribution. NACA TN No. 708, 1939.

7. Glauert, H.: The Effect of Compressibility on the Lift of an Aerofoil. R. & M. No. 1135, British A.R.C., 1927.

8. Prandtl, L.: General Considerations on the Flow of Compressible Fluids. NACA TM No. 805, 1936.

9. von Kármán, Th.: Compressibility Effects in Aerodynamics. Jour. Aero. Sci., vol. VIII, no. 9, July 1941, pp. 337-356.

10. Nitzberg, Gerald E.: The Effect of Compressibility on Two-Dimensional Tunnel-Wall Interference for a Symmetrical Airfoil. NACA ARR No. 3E28, 1943.

11. von Kármán, Th., and Tsien, H. S.: Boundary Layer in Compressible Fluids. Jour. Aero. Sci., vol. V, no. 6, April 1938, pp. 227-232.

12. Glauert, H.: The Elements of Aerofoil and Airscrew Theory. Univ. Press, Cambridge, 1926.

13. Theodorsen, Theodore: On the Theory of Wing Sections with Particular Reference to the Lift Distribution. NACA Rep. No. 383, 1931.

14. Stack, John: The N.A.C.A. High-Speed Wind Tunnel and Tests of Six Propeller Sections. NACA Rep. No. 463, 1933.

15. Jacobs, Eastman N., Ward, Kenneth E., and Pinkerton, Robert M.: The Characteristics of 78 Related Airfoil Sections from Tests in the Variable-Density Wind Tunnel. NACA Rep. No. 460, 1933.

16. Jacobs, Eastman N., and Sherman, Albert: Airfoil Section Characteristics as Affected by Variations of the Reynolds Number. NACA Rep. No. 586, 1937.

17. Fage, A.: On the Two-Dimensional Flow past a Body of Symmetrical Cross-Section Mounted in a Channel of Finite Breadth. R. & M. No. 1223, British A.R.C., 1929.

18. Whittaker, E. T., and Watson, G. N.: Modern Analysis. Univ. Press, Cambridge, 4th ed., repr., 1940.

TABLE I.- VALUES OF Λ FOR VARIOUS BASE PROFILES

$\frac{t}{c} = 0.XX$	Rankine oval	Ellipse	Joukowski section	Conventional NACA sections - 00XX	NACA low-drag sections											
					07-0XX	16-0XX	18-0XX	19-0XX	27-0XX	35-0XX	45-0XX	63-0XX	64-0XX	65-0XX	66-0XX	67-0XX
0.06	-----	0.127	-----	0.111	0.125	0.119	0.124	0.127	0.119	0.107	0.106	0.101	0.106	0.109	0.117	0.119
.09	0.236	.196	0.155	.172	.190	.183	.189	.195	.185	.159	.157	.148	.158	.163	.174	.178
.12	.320	.269	.212	.237	.264	.253	.263	.271	.256	.217	.214	.201	.215	.221	.236	.243
.15	.403	.345	.273	.305	.342	.326	.341	.353	.330	.281	.278	.257	.276	.283	.301	.311
.18	.493	.425	.337	.376	.425	.404	.424	.439	.408	.348	.344	.316	.338	.348	.368	.379
.21	.580	.508	.404	.450	.512	.484	.511	.529	.489	.417	.415	.378	.402	.414	.436	.450
.25	.703	.625	.497	.554	.632	.596	.631	.654	.602	.512	.513	.460	.487	.501	.526	.543
.30	.864	.780	.626	-----	-----	-----	-----	-----	-----	-----	-----	-----	-----	-----	-----	-----
.35	1.049	.945	.767	-----	-----	-----	-----	-----	-----	-----	-----	-----	-----	-----	-----	-----
.50	1.690	1.500	1.258	-----	-----	-----	-----	-----	-----	-----	-----	-----	-----	-----	-----	-----
1.00	4.000	4.000	-----	-----	-----	-----	-----	-----	-----	-----	-----	-----	-----	-----	-----	-----

TABLE II.- COMPRESSIBILITY FACTORS FOR CORRECTION EQUATIONS

M'	$\frac{1}{\left[1-(M')^2\right]^{1/2}}$	$\frac{1}{1-(M')^2}$	$\frac{1}{\left[1-(M')^2\right]^{3/2}}$	$\frac{1-0.7(M')^2}{\left[1-(M')^2\right]^{3/2}}$	$\frac{1+0.2(M')^2}{\left[1-(M')^2\right]^{3/2}}$	$\frac{1+0.4(M')^2}{\left[1-(M')^2\right]^{3/2}}$	$\frac{2-(M')^2}{\left[1-(M')^2\right]^{3/2}}$	$\frac{3-0.6(M')^2}{\left[1-(M')^2\right]^{3/2}}$	$\frac{\left[1-0.7(M')^2\right]\left[1+0.4(M')^2\right]}{1-(M')^2}$	$\frac{\left[1+0.2(M')^2\right]\left[1+0.4(M')^2\right]}{1-(M')^2}$	$\frac{\left[2-(M')^2\right]\left[1+0.4(M')^2\right]}{1-(M')^2}$
0.200	1.021	1.042	1.063	1.033	1.072	1.080	2.084	3.164	1.029	1.067	2.074
.300	1.048	1.099	1.152	1.079	1.173	1.194	2.200	3.394	1.067	1.159	2.174
.400	1.091	1.191	1.299	1.154	1.341	1.382	2.390	3.772	1.125	1.307	2.331
.500	1.155	1.333	1.540	1.270	1.617	1.694	2.694	4.388	1.210	1.540	2.566
.550	1.197	1.434	1.717	1.353	1.821	1.925	2.914	4.839	1.267	1.705	2.728
.600	1.250	1.563	1.953	1.461	2.094	2.234	3.203	5.437	1.337	1.916	2.931
.625	1.281	1.641	2.102	1.527	2.266	2.430	3.383	5.814	1.379	2.046	3.054
.650	1.316	1.732	2.279	1.605	2.471	2.664	3.595	6.258	1.426	2.195	3.193
.675	1.355	1.837	2.489	1.696	2.716	2.943	3.845	6.788	1.479	2.369	3.354
.700	1.400	1.961	2.746	1.804	3.015	3.284	4.146	7.430	1.541	2.575	3.541
.725	1.452	2.108	3.061	1.935	3.382	3.704	4.513	8.217	1.613	2.819	3.761
.750	1.512	2.286	3.456	2.095	3.845	4.234	4.968	9.201	1.697	3.115	4.025
.775	1.582	2.504	3.962	2.297	4.438	4.914	5.545	10.46	1.800	3.478	4.346
.800	1.667	2.778	4.630	2.556	5.222	5.815	6.296	12.11	1.926	3.936	4.745
.820	1.747	3.052	5.333	2.823	6.050	6.767	7.080	13.85	2.050	4.395	5.142
.840	1.843	3.397	6.260	3.168	7.143	8.026	8.103	16.13	2.204	4.970	5.637
.860	1.960	3.840	7.526	3.630	8.639	9.752	9.486	19.24	2.400	5.712	6.272
.880	2.105	4.433	9.333	4.273	10.78	12.22	11.44	23.66	2.659	6.705	7.116
.900	2.294	5.263	12.08	5.229	14.03	15.99	14.37	30.36	3.018	8.098	8.293
.910	2.412	5.817	14.03	5.897	16.36	18.68	16.44	35.12	3.255	9.026	9.076
.920	2.552	6.511	16.61	6.770	19.43	22.24	19.16	41.40	3.552	10.19	10.05
.930	2.721	7.402	20.14	7.946	23.62	27.10	22.86	49.96	3.931	11.69	11.31

TABLE XII

VALUES OF P_e AT STANDARD CHORDWISE STATIONS

x/c	P_e	x/c	P_e
0	0	0.40	1.2475
0.005	0.1796	0.45	1.2669
0.0075	0.2198	0.50	1.2732
0.0125	0.2830	0.55	1.2669
0.025	0.3976	0.60	1.2475
0.050	0.5550	0.65	1.2146
0.075	0.6707	0.70	1.1670
0.10	0.7639	0.75	1.1027
0.15	0.9093	0.80	1.0186
0.20	1.0186	0.85	0.9093
0.25	1.1027	0.90	0.7639
0.30	1.1670	0.95	0.5550
0.35	1.2146	1.00	0

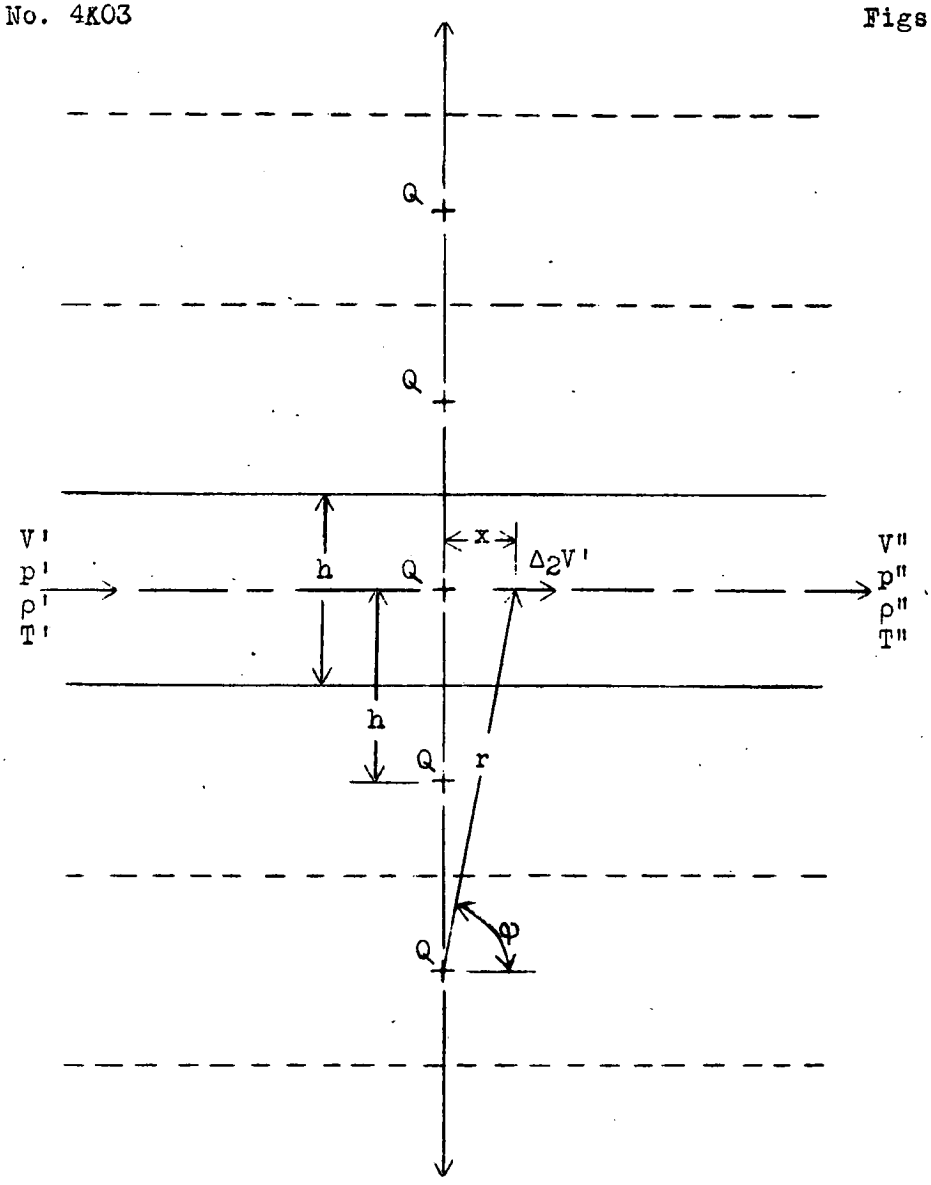

Figure 1.- Source system for analysis of wake effect.

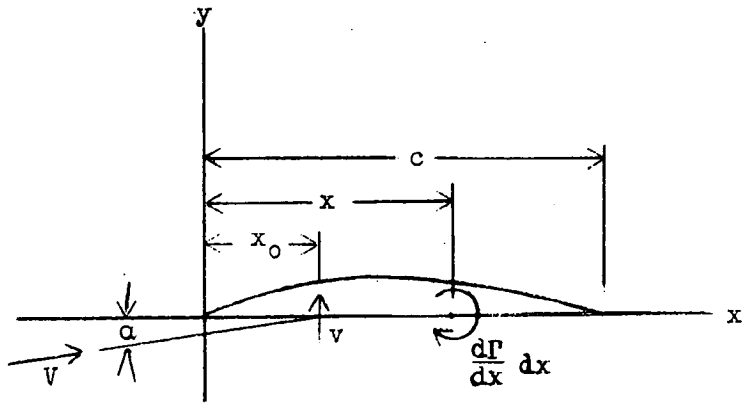

Figure 2.- Mean-camber line in free air.

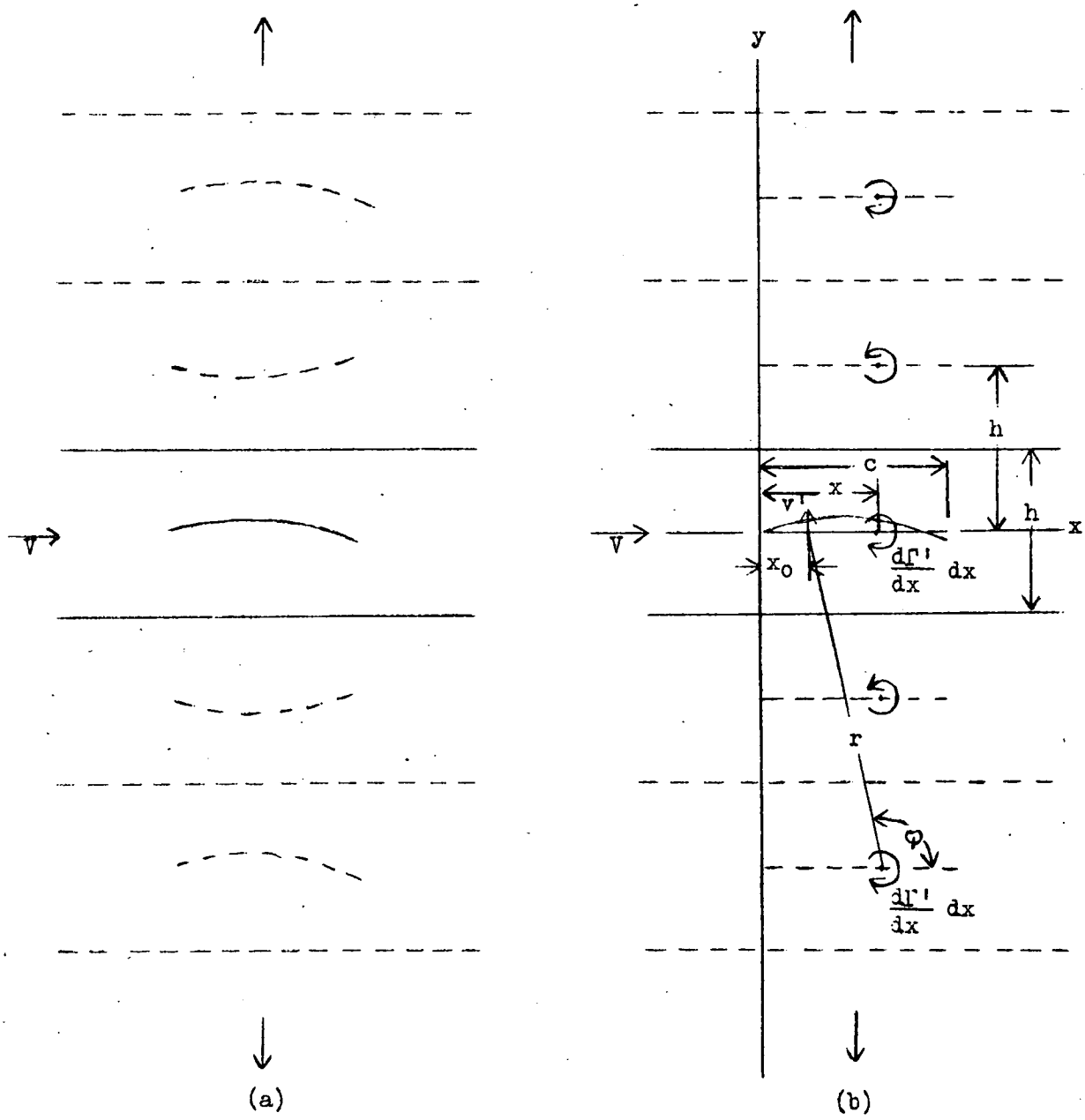

Figure 3.- Mean-camber line in tunnel.

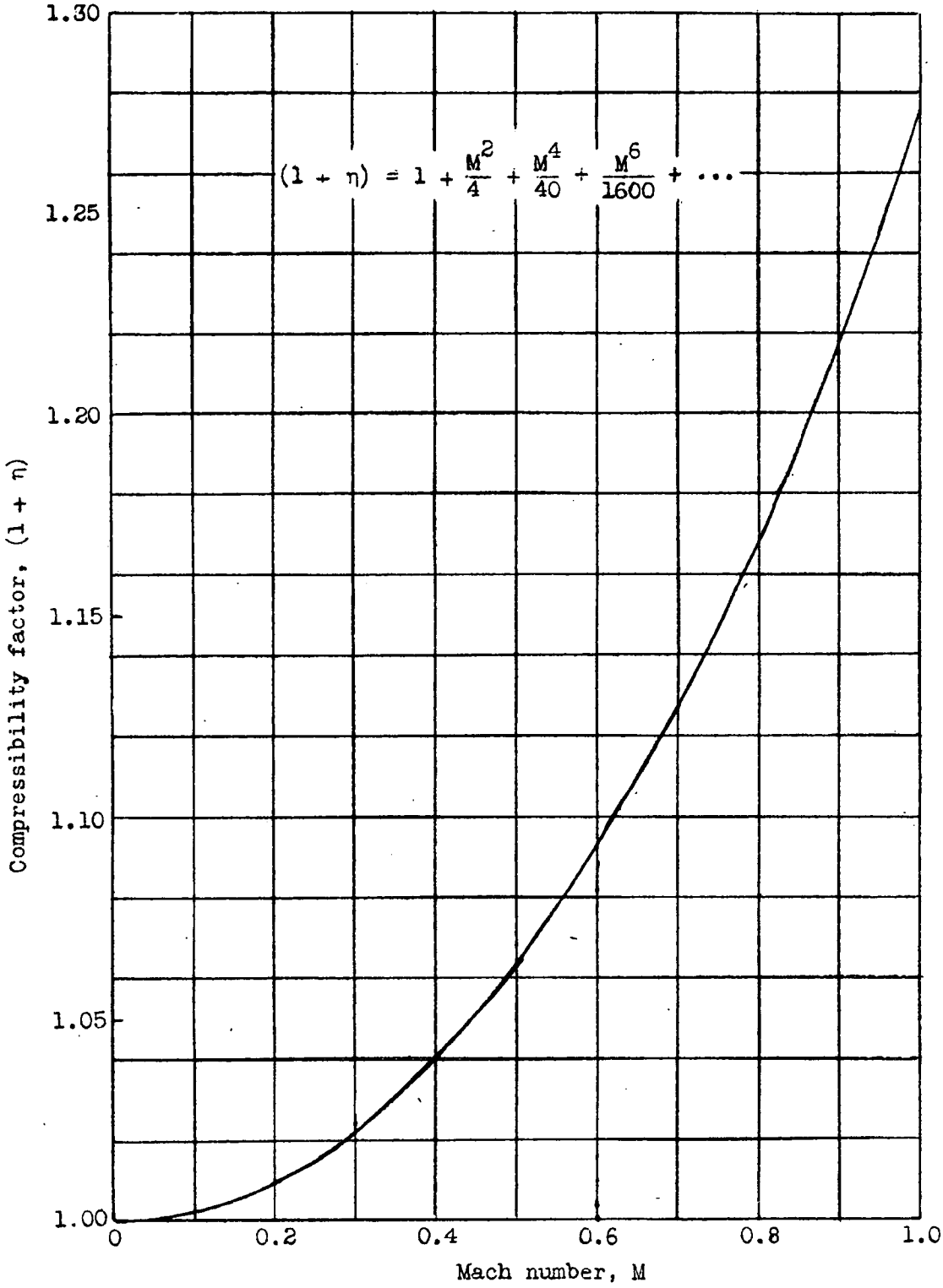

Figure 4.- Compressibility factor.

A-63

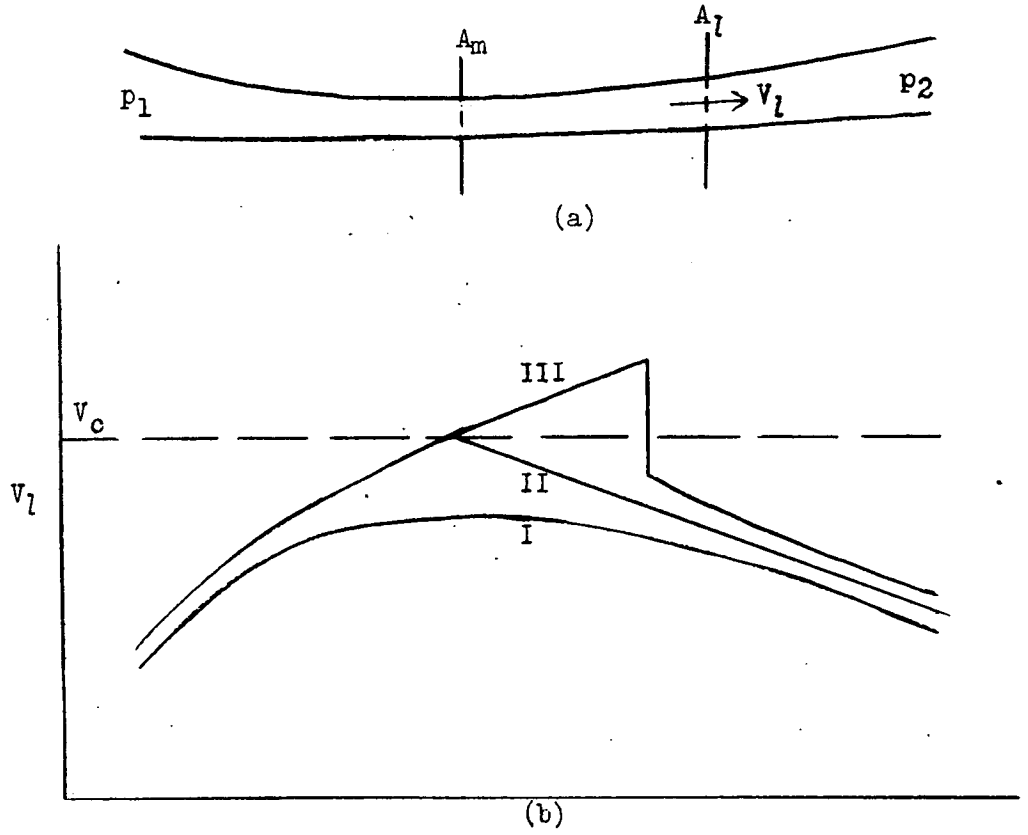

Figure 5.- Velocity distribution in an elementary stream tube.

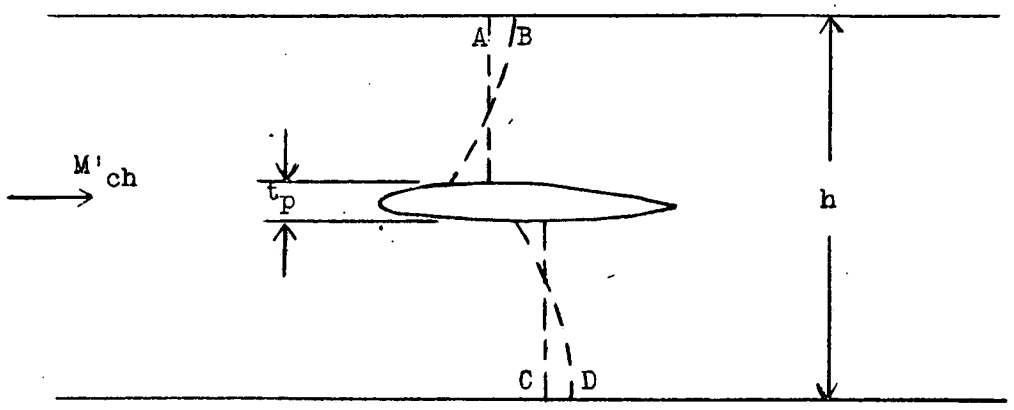

Figure 6.- Lines of sonic speed at the position of the airfoil after choking.

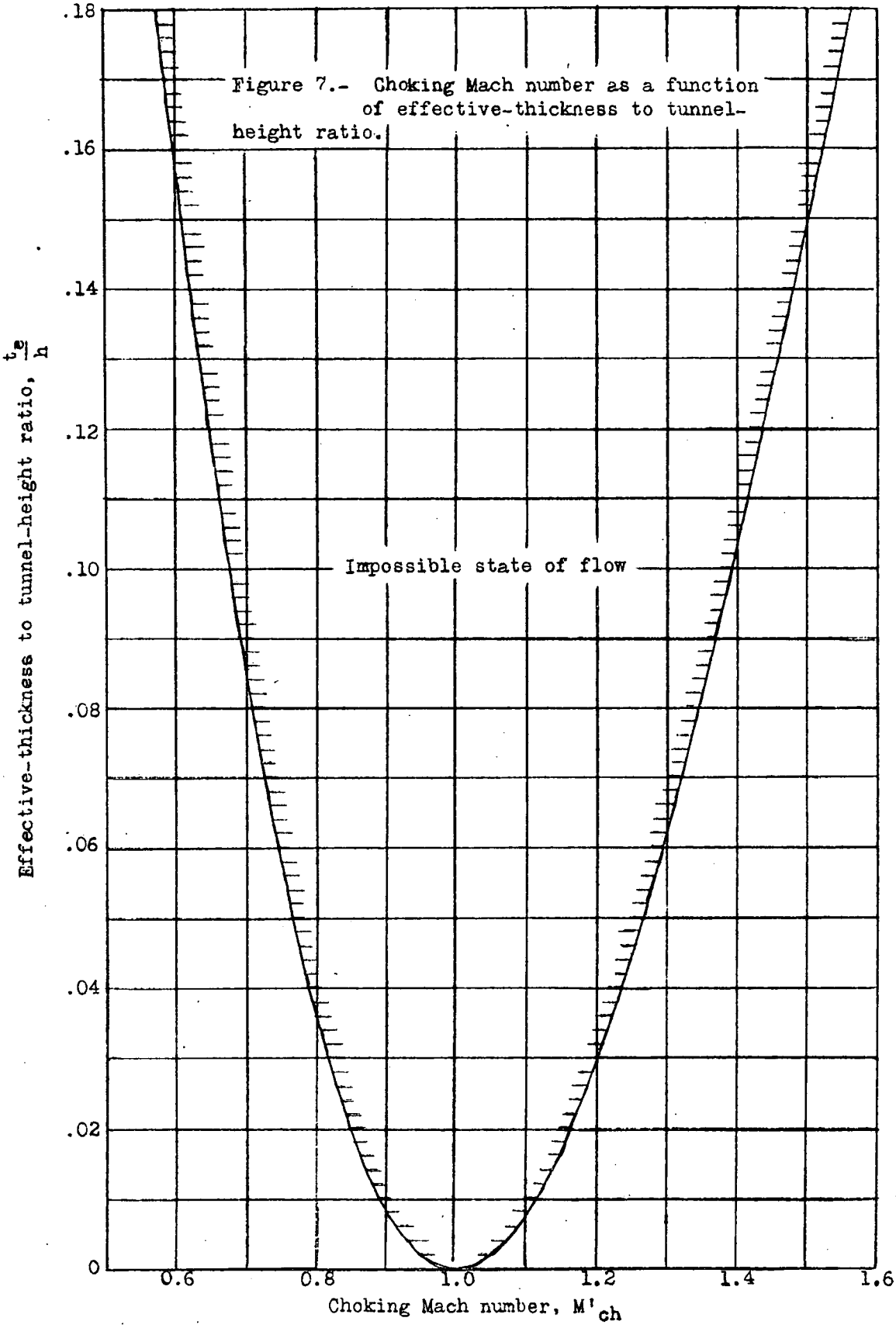

Figure 7.- Choking Mach number as a function of effective-thickness to tunnel-height ratio.

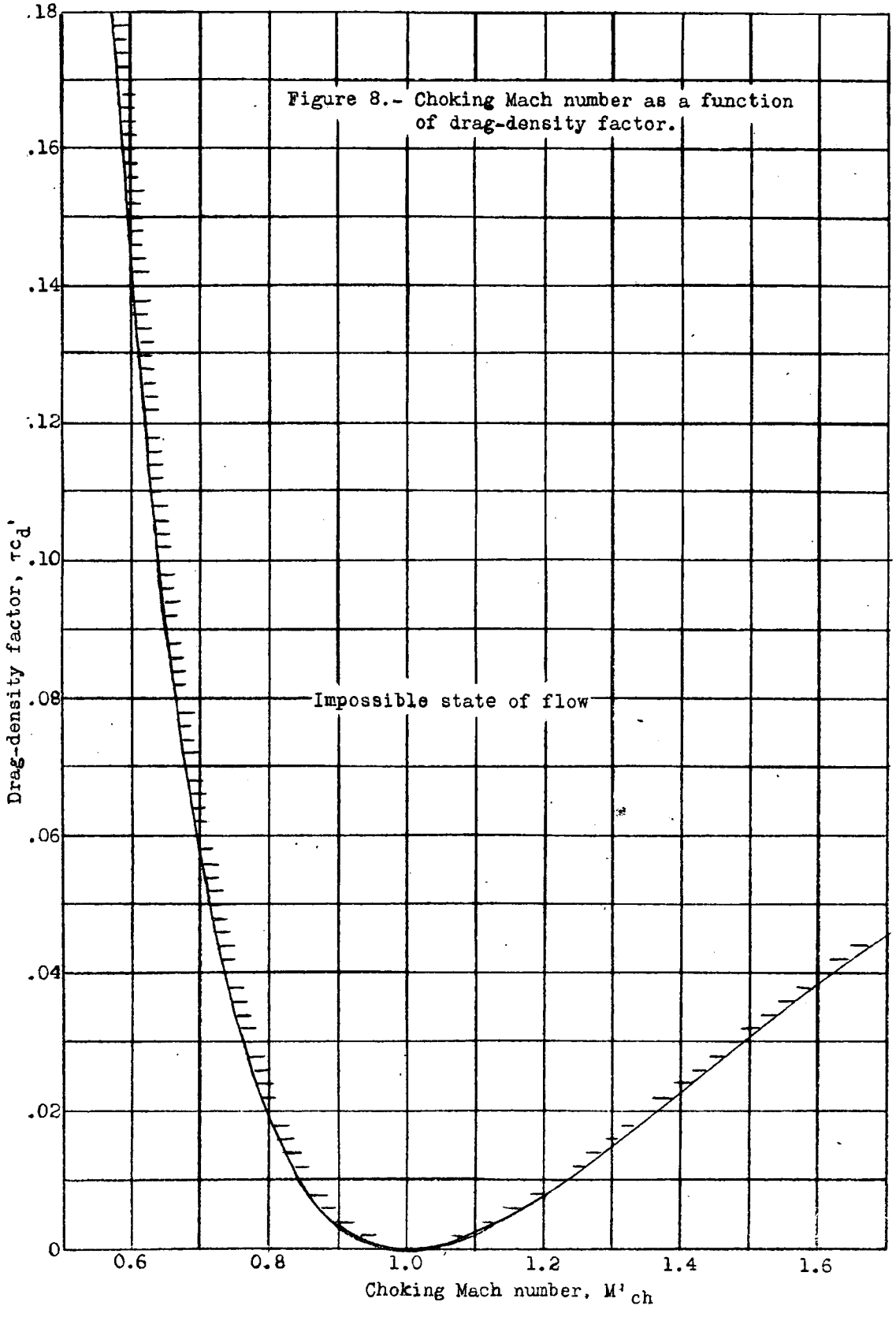

Figure 8.- Choking Mach number as a function of drag-density factor.

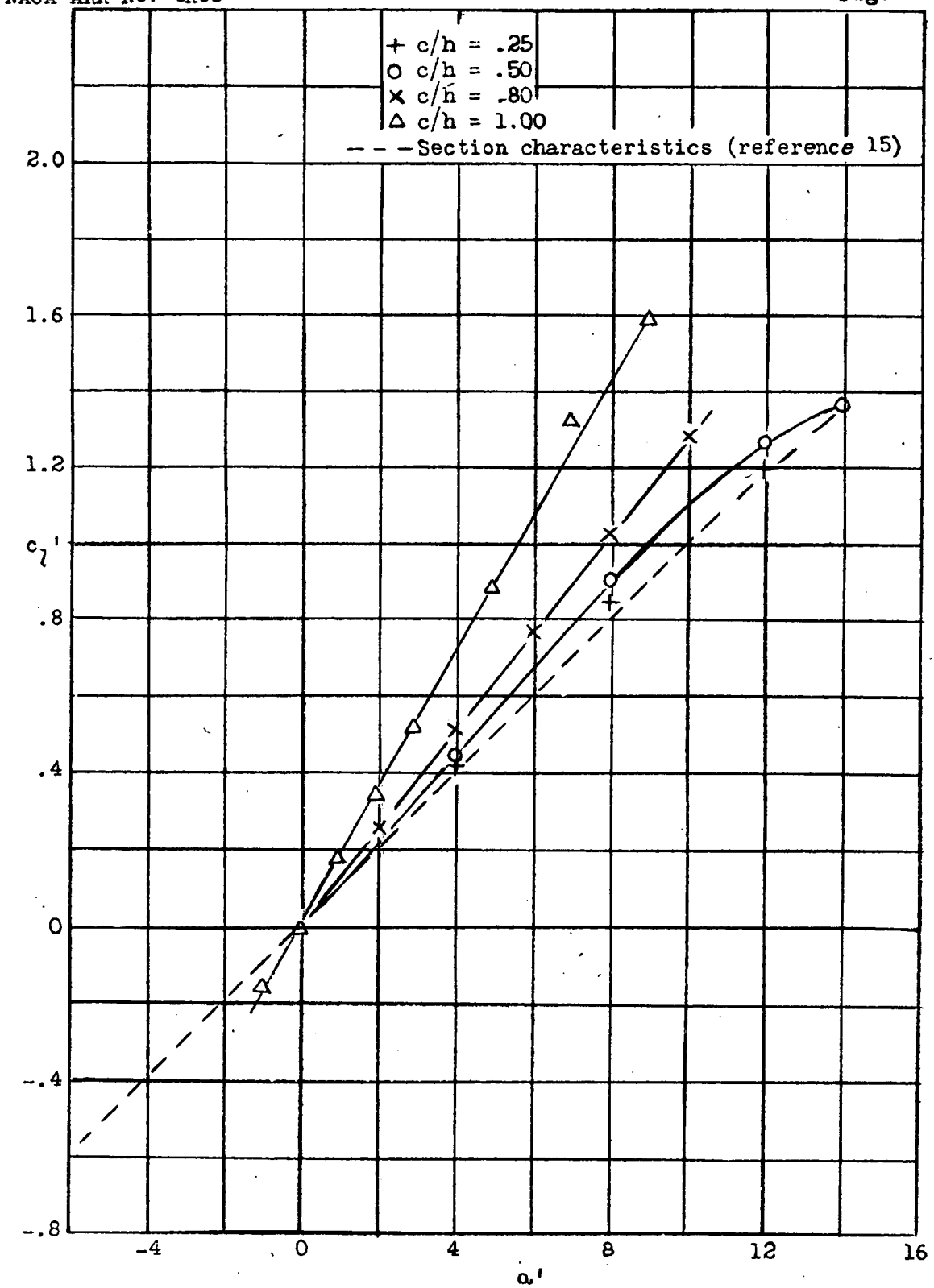

(a) Uncorrected for tunnel-wall interference

Figures 9a,b.- Lift characteristics for NACA 0012 airfoil section.

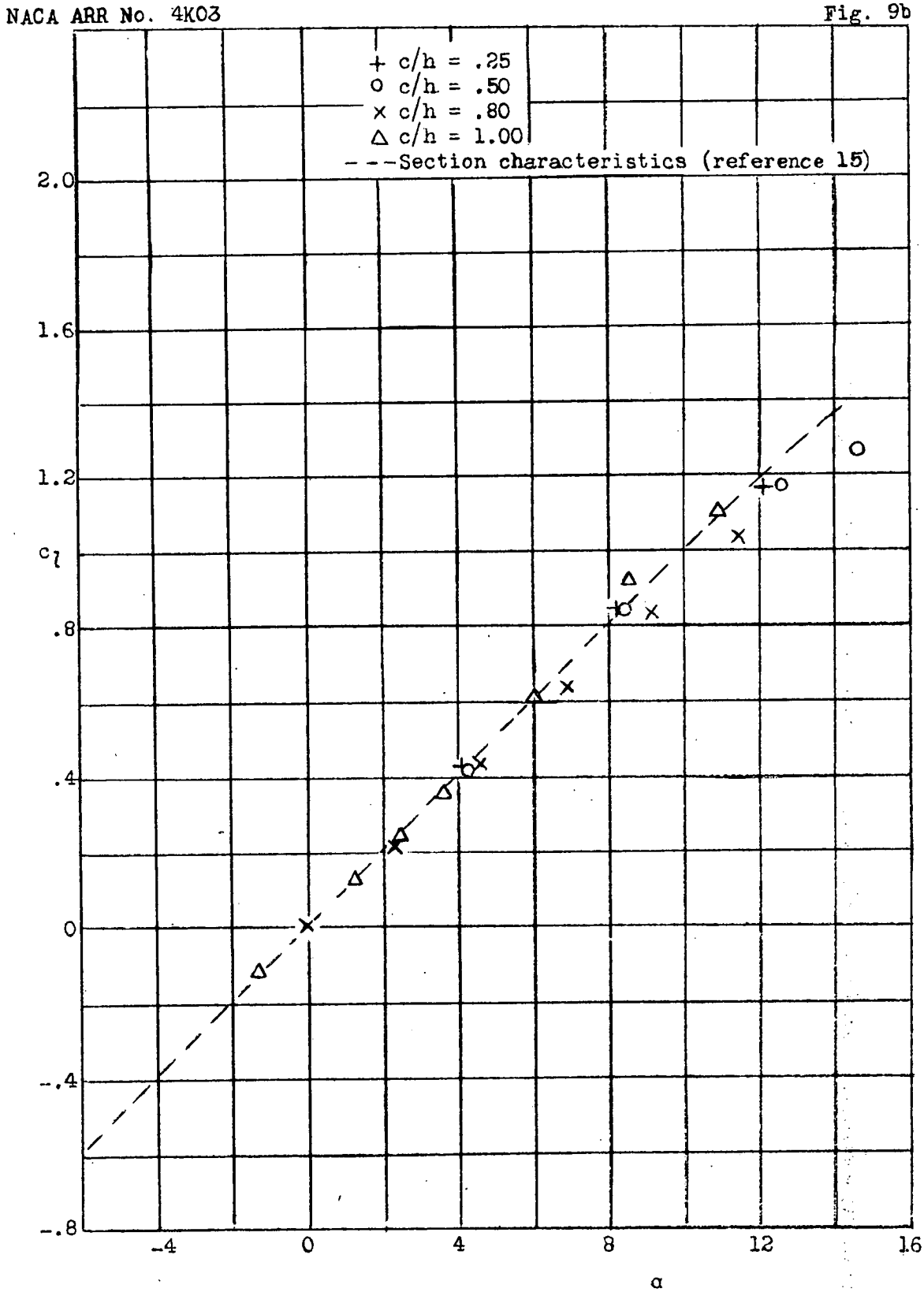

(b) Corrected for tunnel-wall interference

Figure 9b.

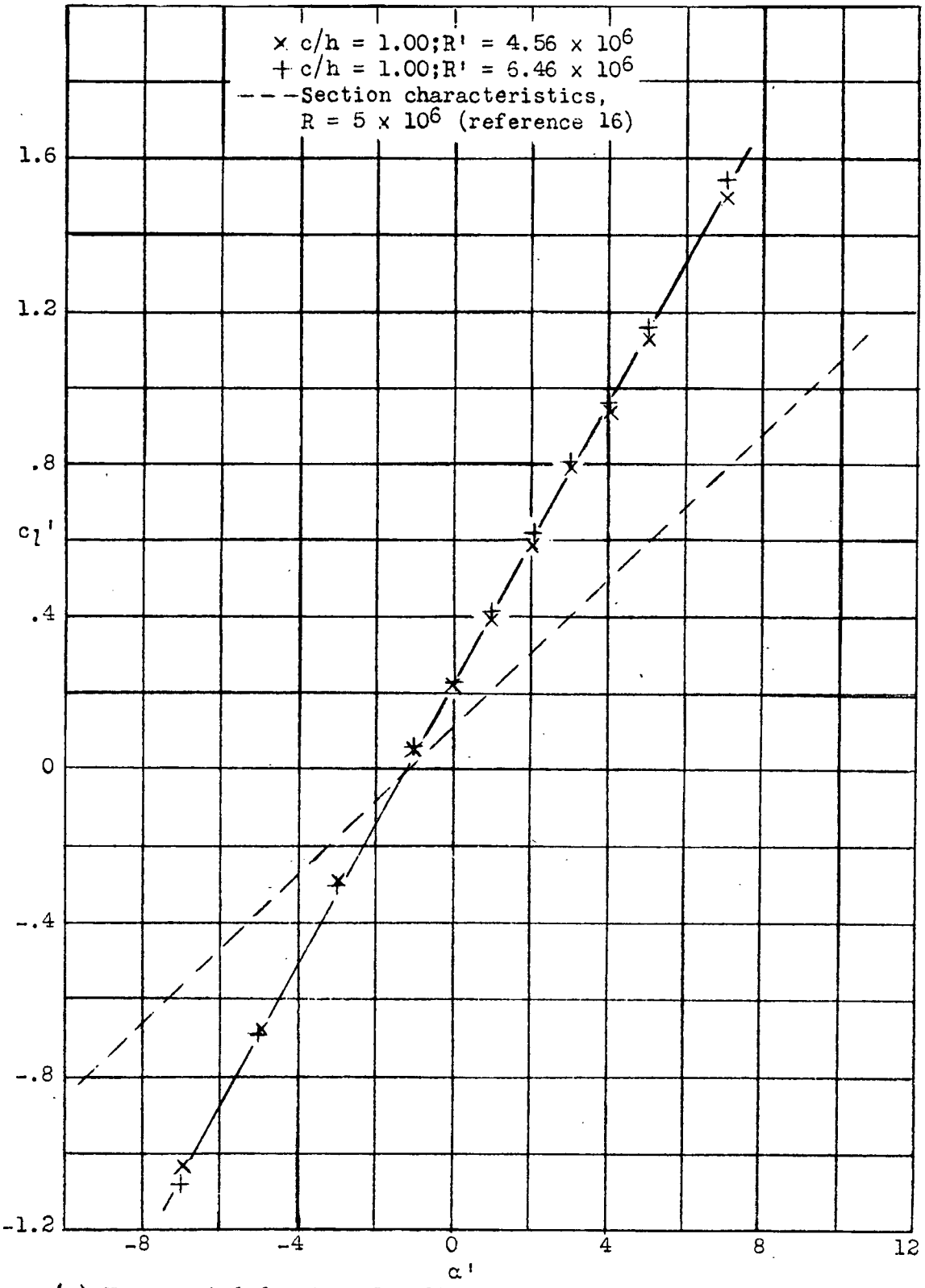

(a) Uncorrected for tunnel-wall interference

Figures 10a,b.- Lift characteristics for NACA 23012 airfoil section

A-63

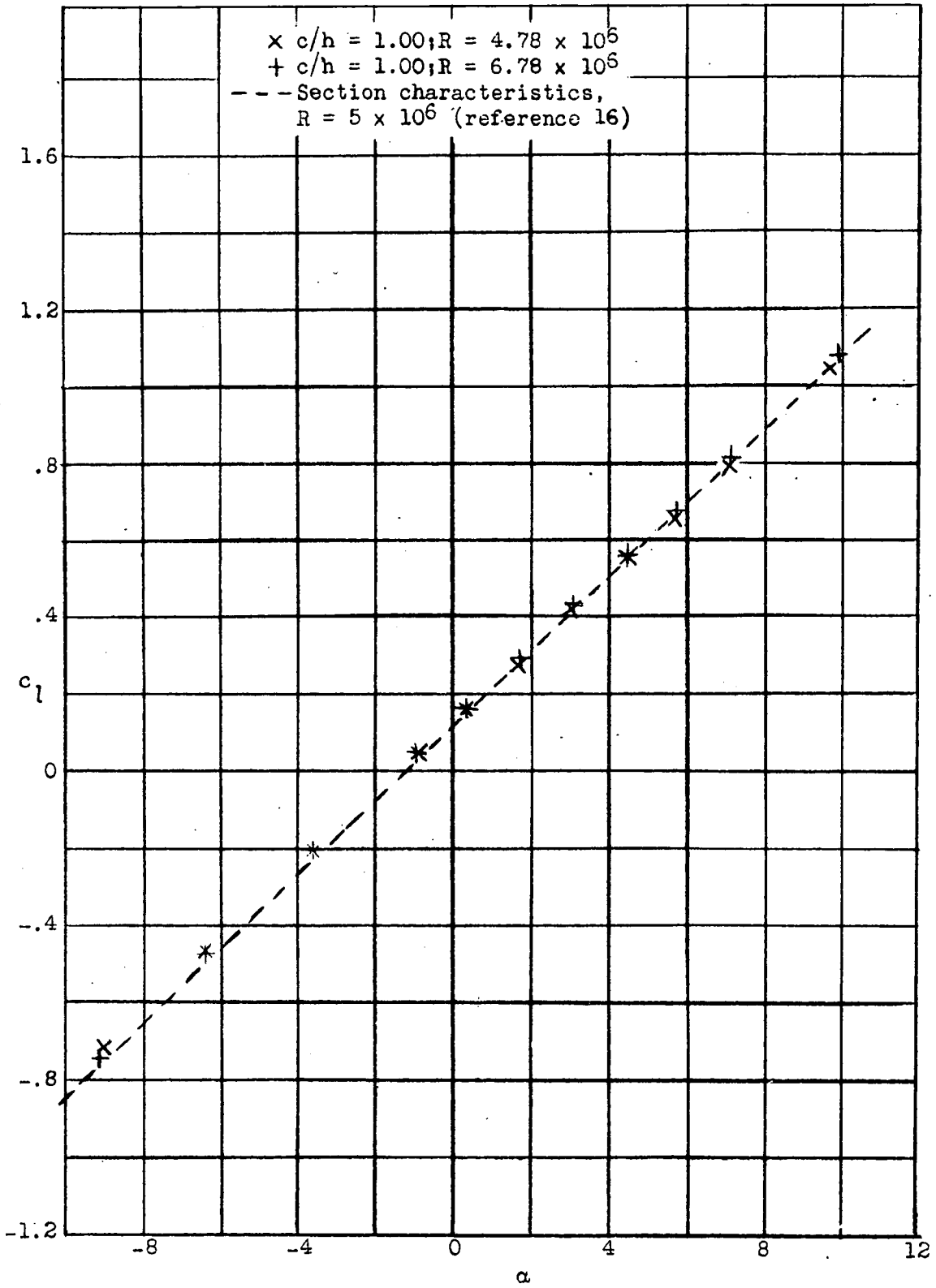

(b) Corrected for tunnel-wall interference

Figure 10b.

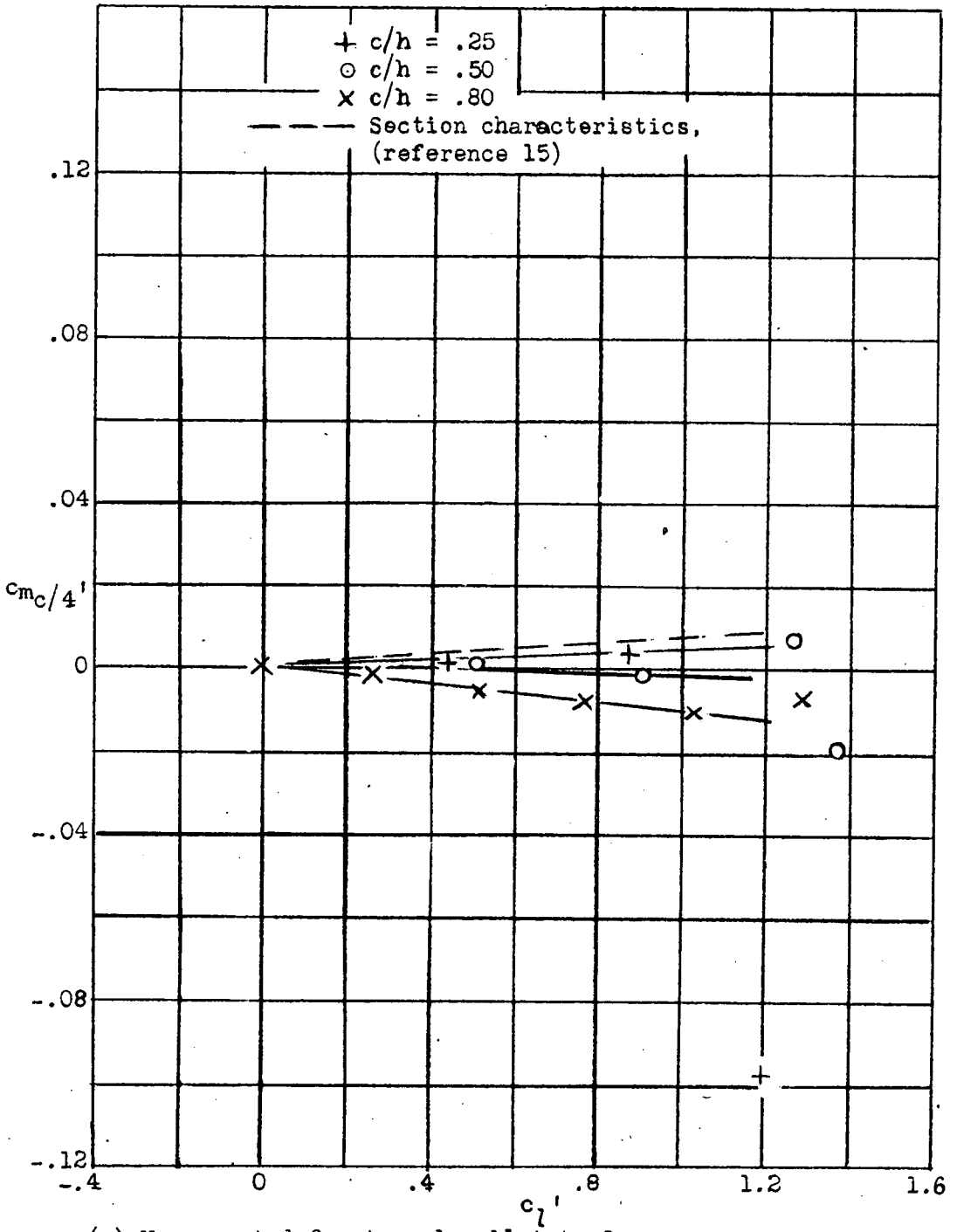

(a) Uncorrected for tunnel-wall interference

Figures 11a,b.- Moment characteristics for NACA 0012 airfoil section.

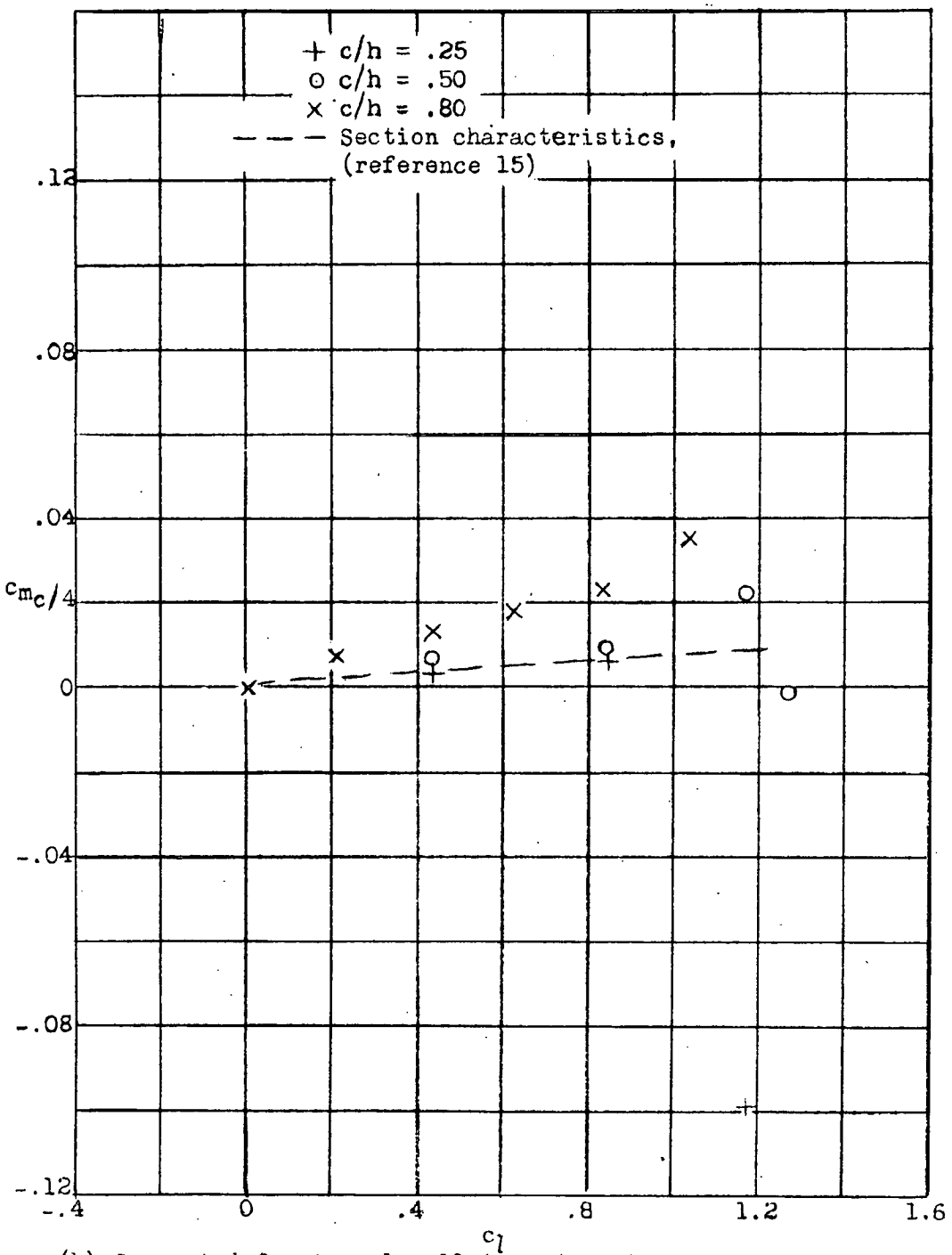

(b) Corrected for tunnel-wall interference

Figure 11b.

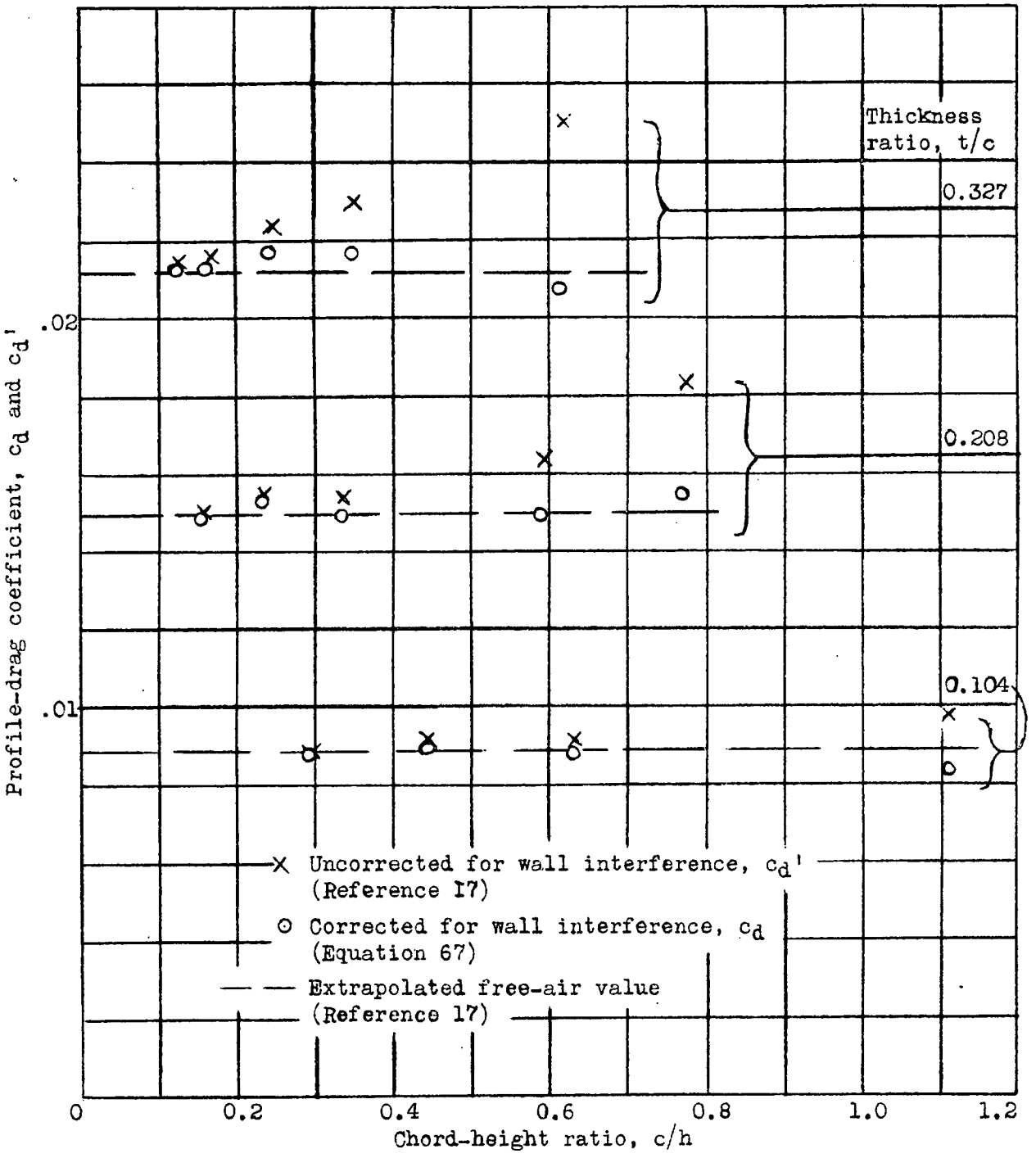

Figure 12.- Profile drag for three symmetrical Joukowski airfoils at zero angle of attack.

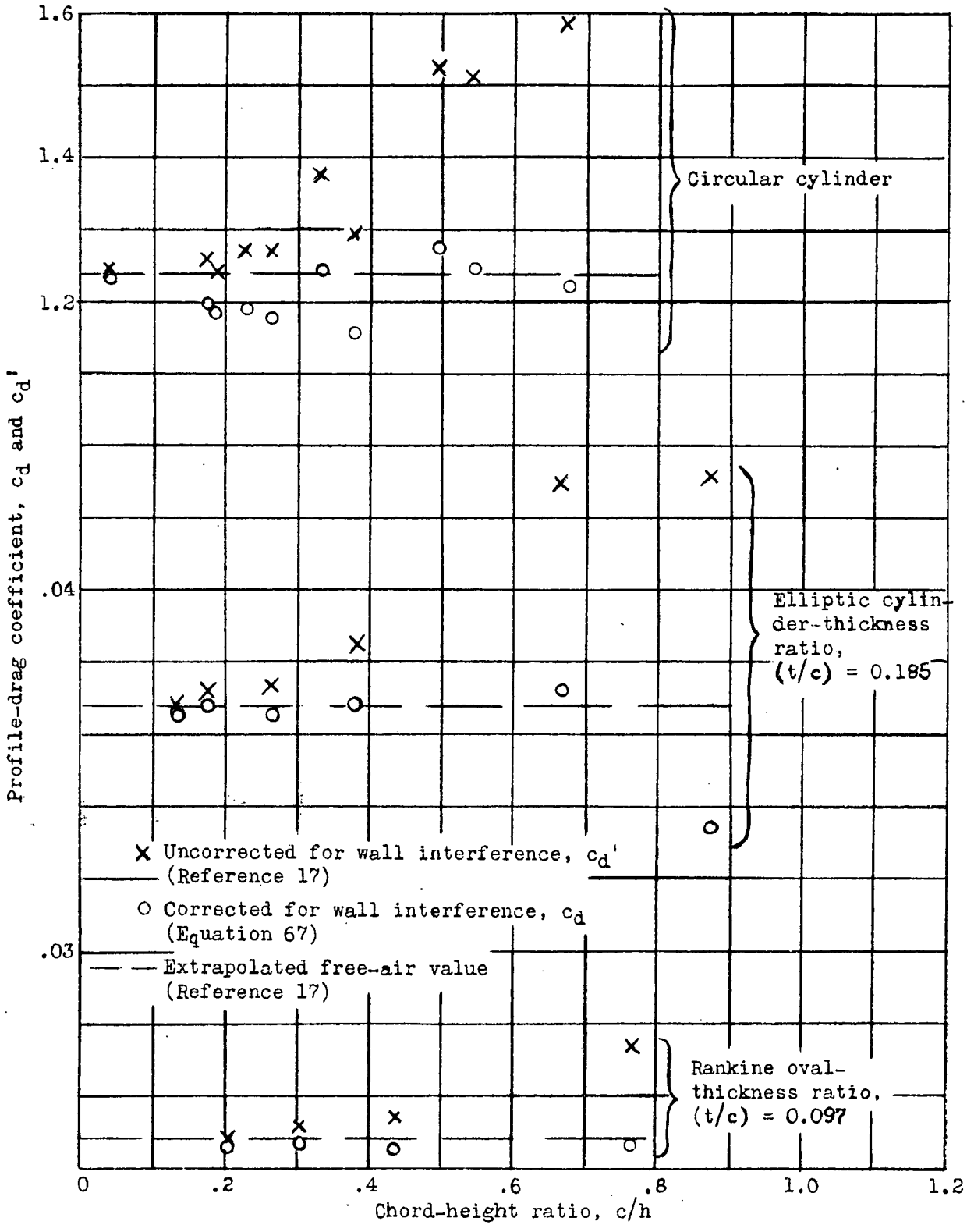

Figure 13.- Profile drag for three symmetrical bodies at zero angle of attack.

A-63

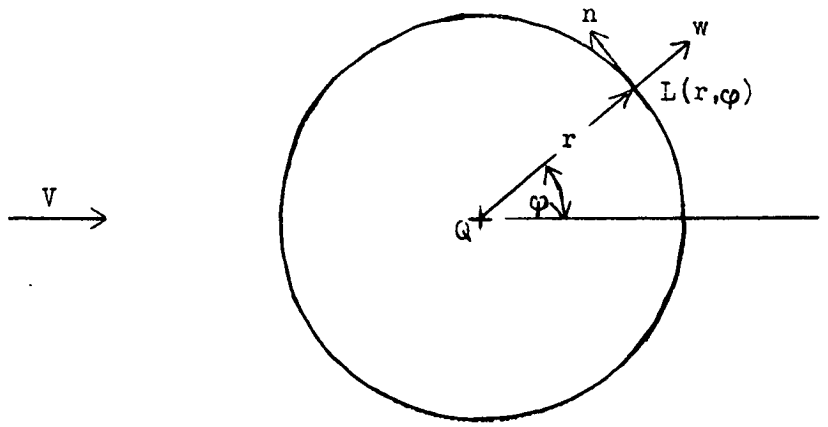

Figure 14.- Velocity induced by a source.

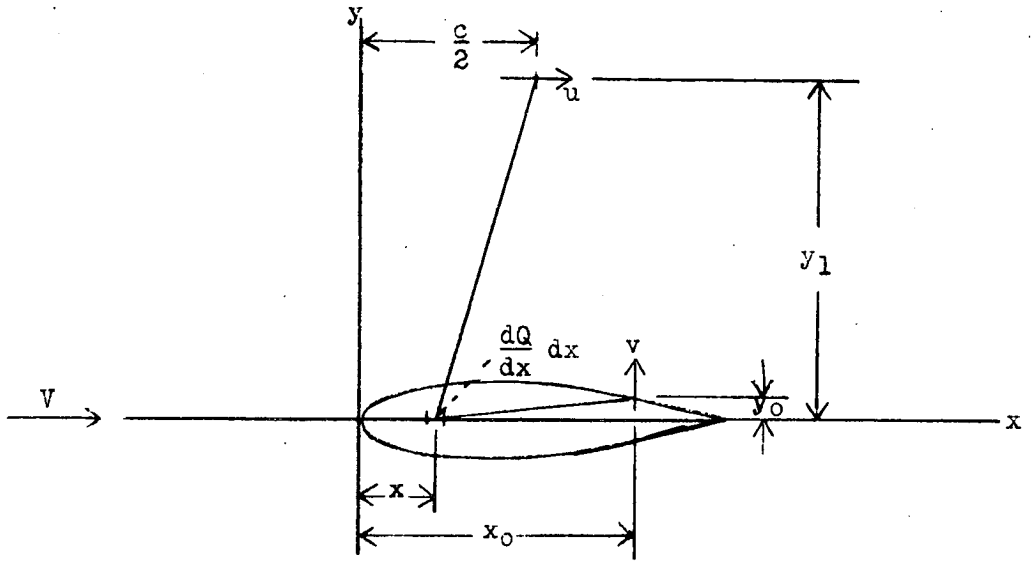

Figure 15.- Velocity induced by a symmetrical airfoil.